POLITECNICO DI MILANO

School of Industrial and Information Engineering

Course of Master's Degree in Electrical Engineering

Influence of Design Parameter on Output Torque of Inset Type Flux Reversal Machine .

Academic tutor : Prof. Antonino DI GERLANDO

Master's degree thesis of
Mohammad Salim Hossain
Student ID: **798166**

Academic Year 2012/2013

INDEX

List of figure

List of Table

Page

ACKNOWLEDGEMENTS

First of all, I would like to express my most sincere gratitude and appreciation to my supervisor, Professor Antonino DI GERLANDO, for his constant and invaluable guidance, inspiration and encouragement throughout these four years. I have learnt a lot from my supervisor – his dedication, attitude and devotion to not only the academic activities but also the way of life.

During these years, a lot of people leave a mark on me and my academic career, and it's thanks to each one of these people that I could become how I am; I can't say thanks to all of us, but I'll try to mention as many names as possible.

Last but not the least, I wish to express my deepest appreciation to my family for their constant understanding and encouragement as well as genuine support. Without these, this work would have been much more difficult. I also thanks to Alauddin and Rakib for tolerating me. Also give thanks to Hanza, Nahian, Saad, Sowad, Naveel, Nabeel and liyana.

Abstract

Due to high efficiency and high power density, permanent magnet (PM) electric machines have been developed and widely accepted for industrial and vehicular applications. Flux reversal machine (FRM) is getting attention for last two decade. It has both permanent magnets and concentrated windings in its stator with reverse PM flux linkage. It can operate in both motoring and generating modes. Its simple structure makes it cost effective and suitable for mass production. However it has few drawbacks such as high cogging torque, notable PM flux linkage. To overcome this drawback FRM with an inset type permanent magnet has been introduce.

My work consisted in carrying out the influence of design parameters of an inset type flux reversal machine for maximum output torque has been investigated by finite element analyses. These parameters include the stator back-iron thickness, the stator tooth width, the rotor pole arc, the rotor back iron thickness, and the rotor pole height.

The outcome of my can be used for design inset type FRM based on the application such as wind power generation, aircraft and automotive.

CAPTER 1

INTRODUCTION

1.1 Introduction

Brushless motors such as brushless DC motors (BLDCM) and switched reluctance motors (SRM) is gaining significant attention in various applications, and a BLDCM is more effective in high efficiency, high power density and compact size. However, in the BLDC motor permanent magnet is placed inside the rotor which makes this motor suffer from the possibility of irreversible demagnetization by armature reaction flux or high temperature. Also, the mechanical integrity of permanent magnets inside the rotor gives this motor a limit in high-speed applications. On the other hand, the absence of permanent magnets in the SRM has some advantages such as simple construction, fault tolerance and mechanical robustness and cost effectiveness as merit but it has lower efficiency, lower power density, control complexity, noise and vibration as a demerit at the same time compared to BLDCMs [1]. High cost of rare earth permanent magnet materials intensifies a need for the combination of an SRM with a BLDCM by slightly adding permanent magnets into the stator of the SRM such as doubly-salient permanent magnet machine (DSPMM) [2], flux-reversal permanent magnet machine [3] and flux-switching permanent magnet machine [4].

Flux Reversal Machine is a new doubly salient stator-permanent magnet machine (with respect to excitation) with flux linkage reversal in the stator winding, which usually is concentrated. While the FRM is not the first DSPMM to have stationary magnets combined with a simple unexcited variable reluctance rotor, it appears to be the first to have bipolar flux and magneto motive force (MMF) variation with rotor position. It has low self and mutual inductances, hence has low electrical time constant [3]. This feature combined with simple construction and low rotor inertia makes FRM attractive as a low cost high speed generator. The first doubly salient stator permanent magnet machine called a flux switch alternator was introduced in 1955. It had poor usage of rotor volume. The stator vibration and difficulty in

manufacturing the stator were viewed as the drawbacks then. In an effort to improve the torque density, to reduce stator vibration, and to simplify the manufacturing process, the first single phase FRM was introduced in 1997. This machine can be used in automobile applications to replace the claw pole alternator which has certain limitations such as limited efficiency and limited ability to respond quickly to sudden load changes.

The flux linkage in any stator coil of FRM varies from a minimum to a maximum value without changing polarity. Flux reversal tends to produce fast flux variation with rotor position and thus large torque is expected for a given stator MMF. A single-phase 2/3 configuration has some advantages, such as a low device count for the power electronics controller and a low frequency of flux-reversal per revolution. It has certain limitations such as an unbalanced magnetic circuit and a high level of noise and vibration arising out of it. In the light of these advantages and disadvantages, it is interesting to consider some other FRM configurations such as a two-phase and a three-phase. In an effort to maintain the advantages of single phase FRM but to reduce the cogging torque, a three phase FRM machine was introduced in 1999 [5]. The disadvantage in the case of multi-phase configuration is that they need a higher number of devices for the power electronic controller as compared to a single phase configuration. On the other hand, they have a balanced magnetic circuit leading to a lower level of cogging torque, noise and vibration . However, there is notable permanent magnet flux leakage (fringing) and cogging torque caused by its structure. This flux leakage deteriorates the power density and torque ability of the FRM. The cogging torque also produces a pulsating torque ripple resulting in vibration and noise that is harmful to the machine performance. To improve the performance and decrease the construction cost of the FRM, a new inset type FRM with permanent magnets parallel to the stator magnet flux lines has been proposed [6]. This thesis work aim to study, the influence of stator and rotor dimensions, such as the stator tooth width, the stator back iron thickness, the rotor pole arc, the rotor pole height, the rotor back iron thickness etc., on the output torque of a FRM machine will be systematically investigated by 2D finite element analyses.

1.2 DOUBLY-SALIENT MACHINES

An electric machine with doubly-salient structure means that there are salient poles in both stator and rotor. Here, the term “salient-pole” only refers to the practical tooth structure made of iron lamination, but not involves the salient-pole effect generated by other means. In a common used term “*x*/*y*-pole” to describe a doubly-salient machine, *x* and *y* denote the numbers of salient poles in stator and rotor respectively.

The simplest doubly-salient machine is the switched reluctance (SR) machine, which was firstly systematically proposed by Lawrenson in the early 1980’s [7] and then well explored by in the next two decades . There are various combinations of *x* and *y* for SR machines and the cross-section of a common 6/4-pole one is shown in Fig. 1.1, which is simply composed of a laminative stator, a laminative rotor and armature windings wound on stator poles. The torque of a SR machine is produced by the tendency of its rotor to move to a position where the inductance of the excited winding is maximized. So, in motoring operation, phases are energized in turn when their inductances are increasing and are de-energized when their inductance are decreasing, hence producing a positive torque all the time to drive the rotor.

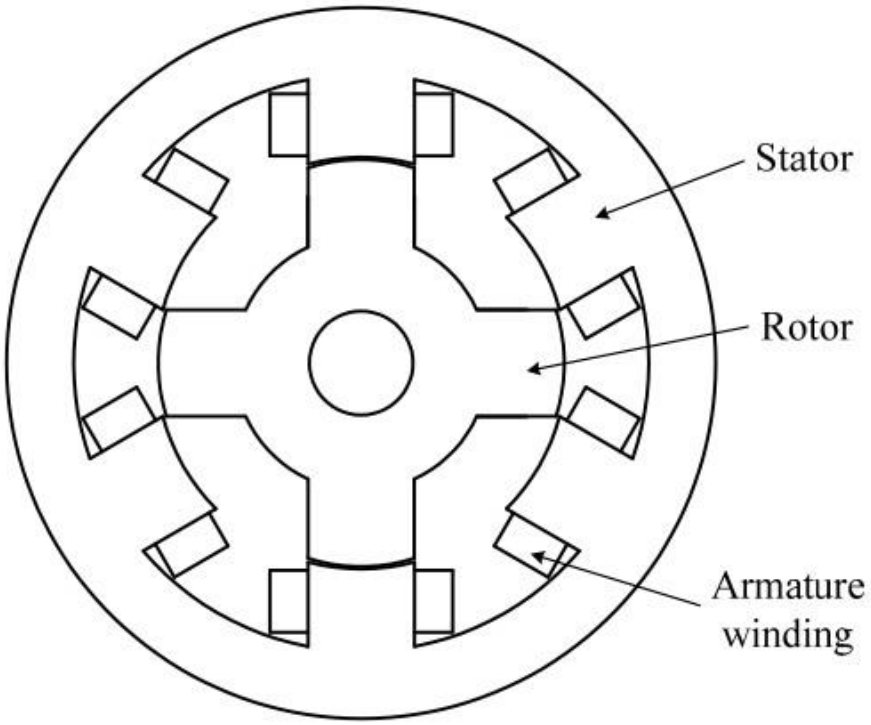

Figure 1.1 Cross-section of a 6/4-pole SR machine.

Although SR machines definitely take the advantages of simple construction, high fault tolerance and mechanical robustness, they also have some apparent deficiencies, such as low efficiency, low power density, and excitation penalty. As a result, researches on the incorporation of additional excitation sources, namely field windings and PMs, into the basic SR machine structure have been inspired.

For the case of incorporating PMs into SR machine, a special version is to mount a pair of PMs between four rotor poles of a 6/4-pole SR machine as illustrated in Fig. 1.2 [8] . The PMs only function to reinforce repulsion torque when they leave the aligned position to stator poles, instead of serving to provide a major excitation source. Hence, this machine is energized by the same manner as that does in the SR machine and is named as the hybrid type SR machine. Except for this special case, all the other PM-incorporated doubly-salient machines have the same operation principle as that of the DFDS machine, and can be divided into rotor-PM type and stator-PM type.

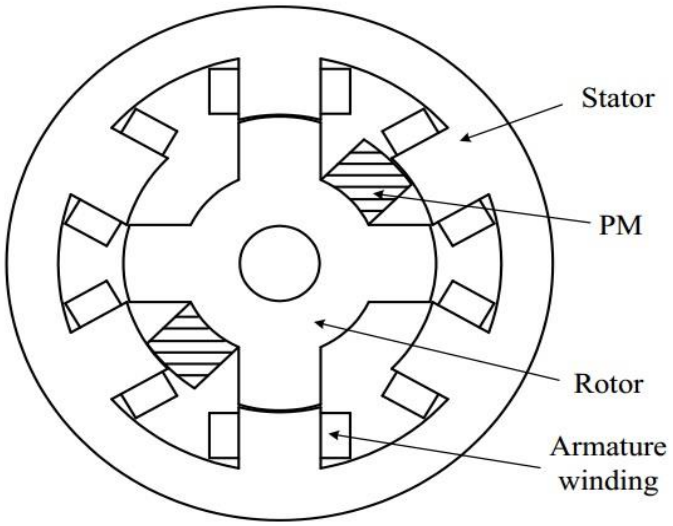

Figure 1. 2 Cross-section of a 6/4-pole hybrid type SR machine.

Fig. 1.3 shows two 6/4-pole doubly-salient machines with rotor-PM, where PMs are placed either in rotor yoke [9] or in rotor poles [10]. However, this rotor-PM type machine is less attractive than the stator-PM type because of its rotary PMs and possible mechanical instability. Hence, most of the researches have turned to the doubly-salient machines with

stationary PMs, which also fall into three categories according to their manner of placement of PMs.

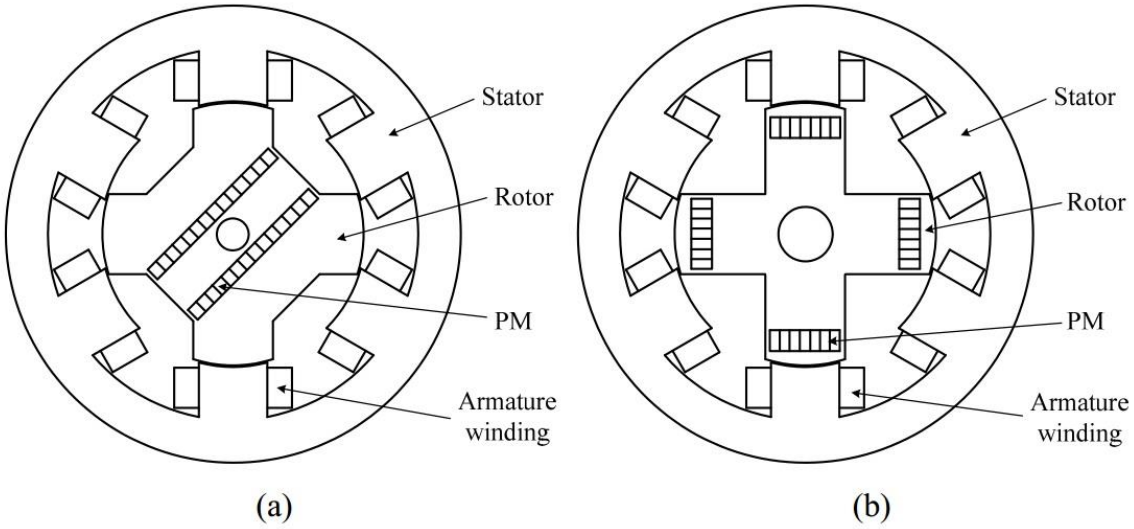

Figure 1.3 : Cross-sections of rotor-PM type DSPM machines. (a) 6/4-pole, PMs in rotor yoke. (b) 6/4-pole, PMs in rotor poles.

1.2.1 Doubly-Salient PM(DSPM)

The first one is to place PMs in the stator yoke and the resulting machine is referred to as doubly-salient PM (DSPM) machine. In fact, the rotor-PM doubly-salient machine is normally categorized as a DSPM machine because of its similar operation principle and trapezoidal back EMF to the stator-PM one. The first DSPM machine with 6/4-pole was proposed and well explored by Lipo in 1992 [11], and he also developed several other topologies of DSPM machines . Then, many other researchers have been involved in the development of the DSPM machines and their motor drives . As the cross-sections of various DSPM machines shown in Fig. 1.4, the most popular and common combinations of stator pole number and rotor pole number are 4/6-pole, 6/4-pole, 8/6- pole and 12/8-pole.

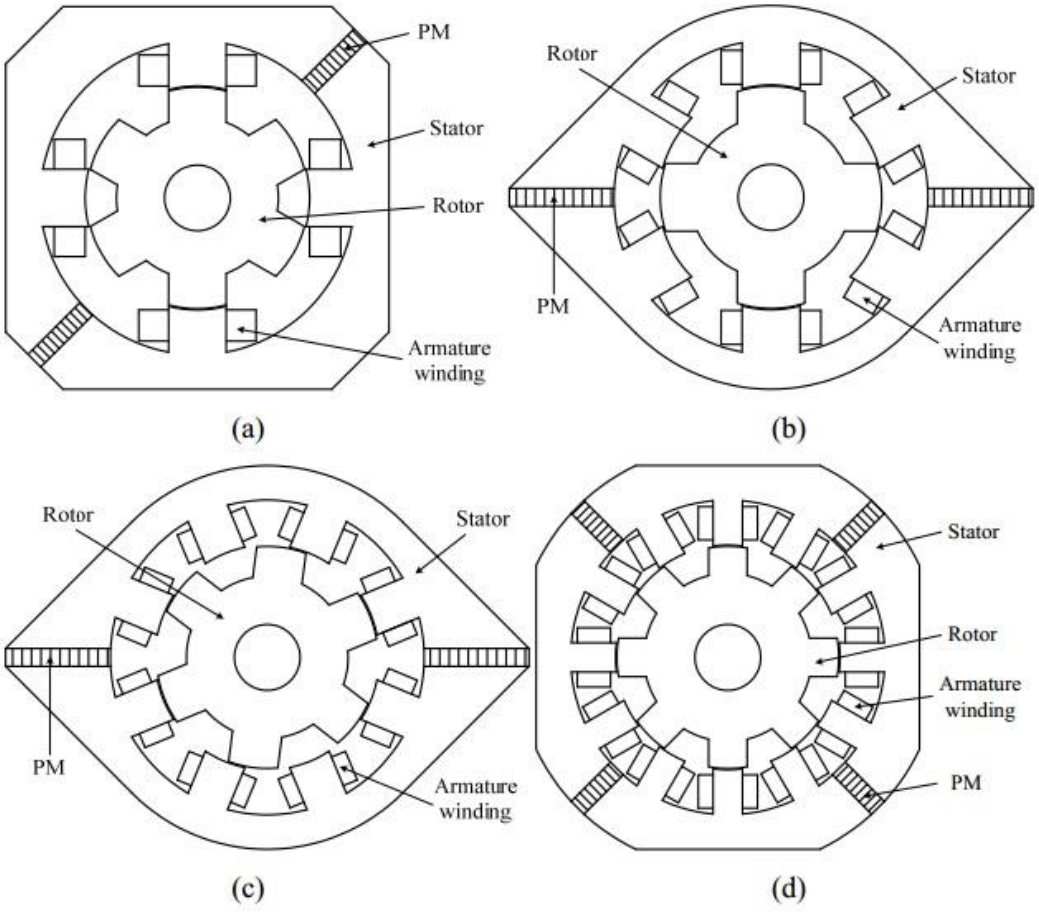

Figure 1.4 *Cross-sections of stator-PM type DSPM machines. (a) 4/6-pole. (b) 6/4-pole. (c) 8/6-pole. (d) 12/8-pole.*

1.2.2 Flux Switching MP (FSPM)

The next one is to mount PMs within the stator poles. The PMs are sandwiched in each stator pole with a circumferential orientation, and the adjacent PMs have the opposite polarity. This machine type termed as flux-switching PM (FSPM) machine was firstly proposed by Hoang in 1997 [4] and well developed in the next decade. Fig. 1.5 shows some different topologies of FSPM machines, where (b) should be regarded as a 6/19-pole version though there are 24 stator teeth. The evolvement process of FSPM machines can be described as follows: two PMs in each stator pole shoe become one, and then further move into the pole towards back iron, and finally settle under the coil; meanwhile, the stator pole shoe disappears. As a result, PMs Immunity from armature reaction and flux focusing is enabled in

the FSPM machine, leading to a significantly high power density. The operation of the FSPM machine is in four quadrants.

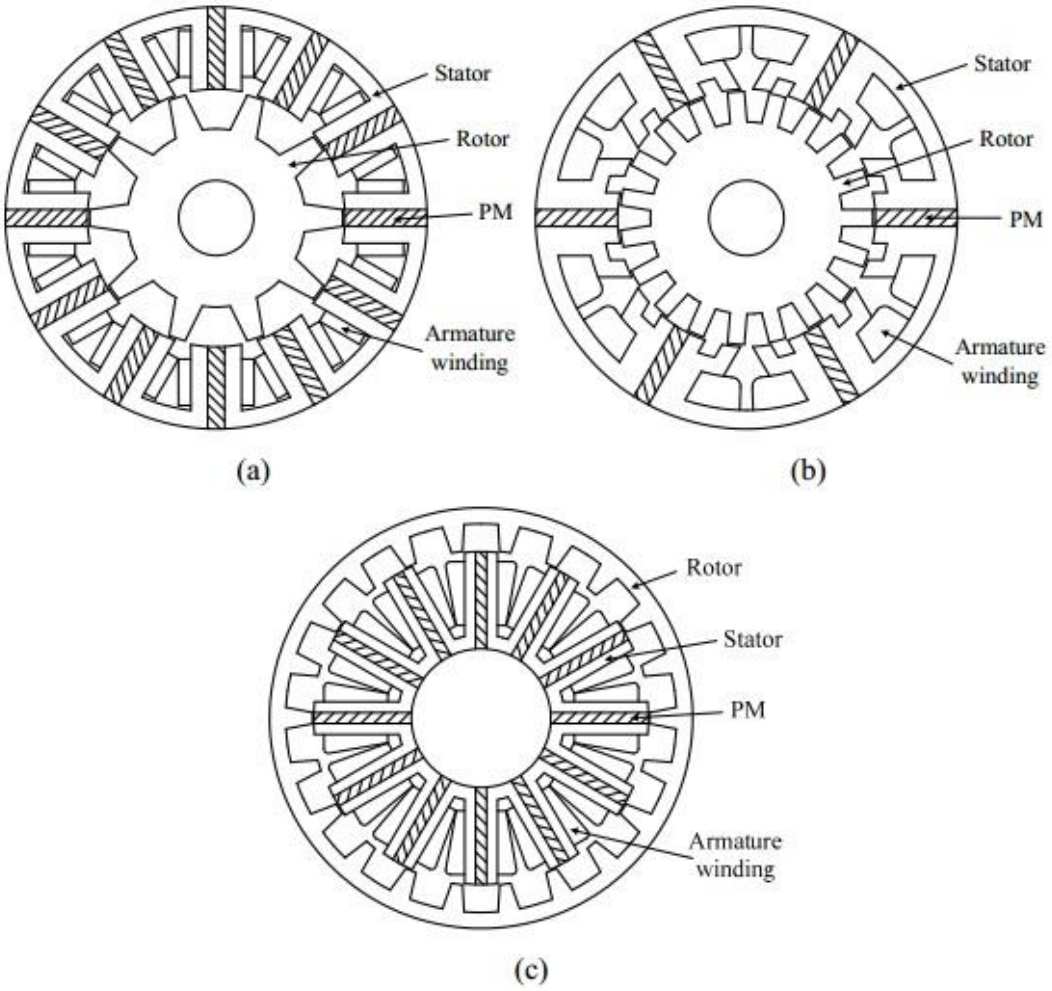

Figure 1.5 *Cross-sections of FSPM machines. (a) 12/10-pole. (b) 6/19-pole, multi-tooth. (c) 12/22-pole, outer-rotor* .

1.2.3 Flux Reversal Machine (FRPM) :

The last one is to place PMs on the stator pole surfaces or in the stator pole shoes, and such a machine is termed as flux-reversal PM (FRPM) machine since the flux linkage with each coil reverses polarity as the rotor rotates. With the advent of the first 2/3-pole FRPM machine in 1997 [12], various machine topologies have been proposed and analyzed, as illustrated in Fig. 1.6, where each stator pole has a pair of PMs of different polarities mounted

onto its surface. The manner of current excitation of FRPM machine is the same as that of the DSPM one; however, rather than unipolar flux linkage in DSPM machines, the FRPM machines have bipolar flux linkages so that the torque density is higher than that of the DSPM machines. Moreover, in order to solve the problem of PMs on the pole surfaces being prone to demagnetization by armature reaction, an improvement has been made in [6] to move PMs into the pole shoes and make them be parallel to the flux lines, as shown in Fig. 1.6(d).

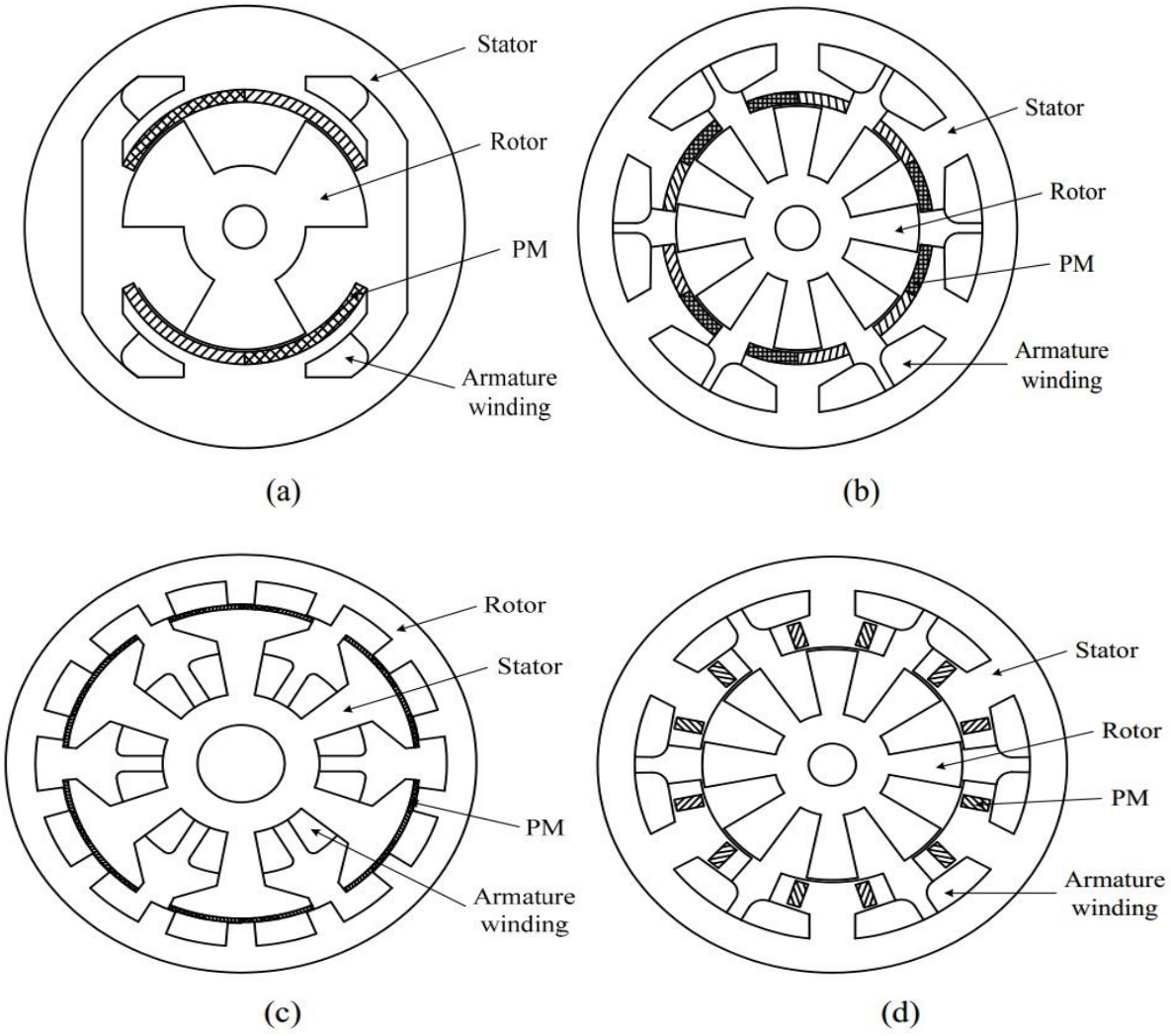

Figure 1.6 Cross-sections of FRPM machines. (a) 2/3-pole. (b) 6/8-pole. (c) 6/14- pole, outer-rotor. (d) 6/8-pole, PMs in stator pole shoes.

In fact, the first doubly-salient machine with stator-PM maybe dates back to 1955. Rauch and Johnson presented such a 4/6-pole machine called the flux-switch alternator, as shown in Fig. 1.7 [13]. But the size of that machine was quite large as only low-energy PM material was available at that time, leading to little attention paid to it for a long time. Although this machine is named as flux-switch, its PMs are placed neither within the stator poles nor on the pole surfaces, but in the stator yoke. However, its flux linkage during operation is bipolar, namely reverse or switched, instead of unipolar of a DSPM machine. So, as a compromise, it is preferred to be named as the FRPM machine [5].

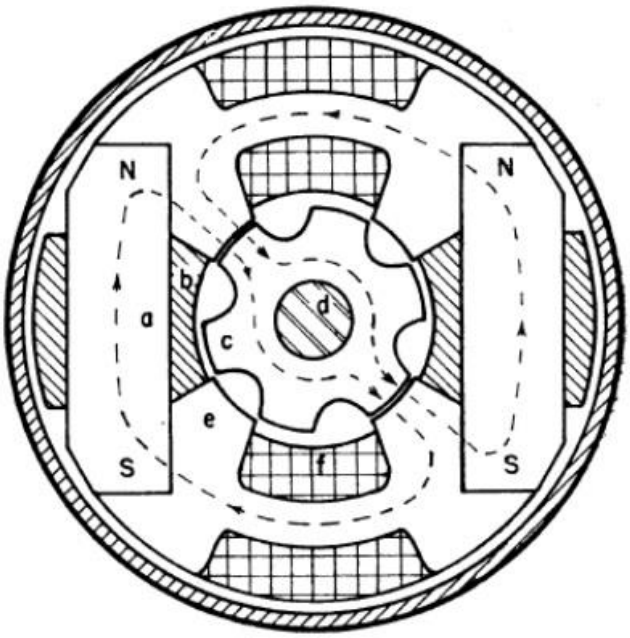

Figure 1.7 *Cross-section of the flux-switch alternator*

a: Ferrite PM b: Magnet shielding c: Rotor d: Nonmagnetic shaft

e: Stator f: Armature winding

Furthermore, a brief comparison among these doubly-salient machines, namely SR, DSPM, FRPM and FSPM, is given as listed in Table 1.1.

Table 1.1 Comparison of different doubly-salient machines

	SR	DSPM	FSPM	FRPM
PMs	No	PMs in Stator or Rotor yoke	PMs within Stator poles	PMS on Stator pole Surface
Field Winding	No	No	No	No
Flux Variation	Unipolar	Unipolar	Bipolar	Bipolar
Current Variation	Unipolar	Bipolar	Bipolar	Bipolar
Back EMF	No	Trapezoidal	Sinusoidal	Sinusoidal
Current	Rectangular	Rectangular	Sinusoidal	Sinusoidal
Energy Conversion Quadrant	First	First and Second	All four	All four
Power Density	Low	High	Very high	Very high
Flux Weakening	NA	Very difficult	Vector Control	Vector Control
Armature Reaction on PMs	NA	Medium	No	High
Cogging Torque	No	Medium	High	High
Manufacture	Simple	Medium	Complicated	Complicated

CHAPTER 2

Flux Reversal Machine (FRM)

2.1 Principle of operation:

Consider an SRM with two stator poles spaced at 180° degrees interval from each other and three rotor poles spaced at 120° interval from each other, with each stator pole having two magnets, and the magnets are attached to the stator poles with the polarities of the PM as shown in Figure 8. The PMs in a stator pole have opposite polarities. The diametrically opposite PMs have the same polarity in the diametrically opposite stator poles. The coils on the stator poles are concentrically wound and they are connected in series to form a single-phase winding and in the present illustration thus constituting a single-phase machine. It is to be stated here that the principle of operation of the FRM under illustration is not limited to single-phase machines and is equally applicable to multiphase machines. [14], [15] explains the rudiments of FRM operation.

Consider the machine windings are not excited and the rotor is driven in the counterclockwise direction. For the rotor position shown in Figure 2.1a, one rotor pole is in the middle of the two PMs in the top stator pole and the PMs in the bottom stator pole each straddle a rotor pole. There are two flux paths, one comprising of the top pole magnets and the top rotor pole with the flux path closing in the back of the stator pole, PMs, air gaps, and rotor pole and the second flux path comprising of the bottom pole magnets and the two remaining rotor poles with the flux path closing with the PMs, back of the stator pole, air gaps, rotor poles, and back iron of the rotor poles. In this position, the fluxes are confined to the stator and rotor poles with no linking of the stator coils, resulting in zero stator flux linkages.

Let the rotor be moved so that the top rotor pole is aligned with the left side PM by moving it from the midpoint of the two PMs. The majority of the flux from the top PM goes through the top air gap, top rotor pole, bottom rotor pole, bottom air gap, bottom stator pole, stator yoke, and back to the top stator pole. This flux divides itself into two paths on either side of the stator yoke as shown in Figure 2.1b. There is also a small leakage flux as shown in the top and the bottom. It may be seen that only one PM in each pole is helpful in producing this change of flux linkage from the previous position to this new position. In between these two positions, it may be assumed that the flux and stator flux linkages are linearly rising. As the center of the rotor pole moves away from the PM, the flux and the stator flux linkages decrease also linearly as per the assumption. From the first position of no flux linkages corresponding to Figure 2.1a and the peak flux linkages corresponding to Figure 2.1b where the center of the PM and the center of the rotor pole in the top aligns, a positive change of flux linkages from zero to maximum is seen. The flux linkages are considered positive by convention as the flux goes from top to down. As the rotor moves away from the top left PM, the flux linkages decrease likewise until they become zero when two rotor poles come under the top pole and they are positioned with each facing a PM of the top stator pole as shown in Figure 2.1c. At this point, the flux is only linking the stator and rotor poles with no flux linking the stator coils.

When two rotor poles come to the top, the bottom pole is centered between the two PMs of the bottom stator pole as shown in Figure 2.1. As the rotor moves, the bottom rotor pole comes more under the right bottom PM, resulting in the flux flow from the bottom magnet in the bottom to top direction through the bottom rotor pole, back rotor iron, the right top rotor pole, air gap, top right PM, and to one of the stator yoke part and back to the bottom stator pole, as shown in Figure 2.1d. This produces the stator flux linkages (negative in direction), which vary with the rotor position with the maximum when the bottom rotor pole aligns with the right PM of the bottom stator pole. When the rotor pole leaves the bottom right PM, the flux linkages are reduced and become zero when the bottom stator pole faces two rotor poles as shown in Figure 8a. Therefore, in one rotor revolution, the stator coils experience three cycles of flux linkages variation with each cycle consisting of a variation from zero to positive maximum, from positive maximum to zero, from zero to negative maximum, and from negative maximum to zero. Bipolar flux with PMs only on the stator poles is uniquely achieved with this machine. Such a stator flux reversal appearing with

magnets on the rotor in conventional PMSMs is to be kept in mind. As the flux reverses in the stator back iron and stator poles with respect to rotor position, these machines may be named as FRMs with stator permanent magnets and for brevity they are referred to as FRM.

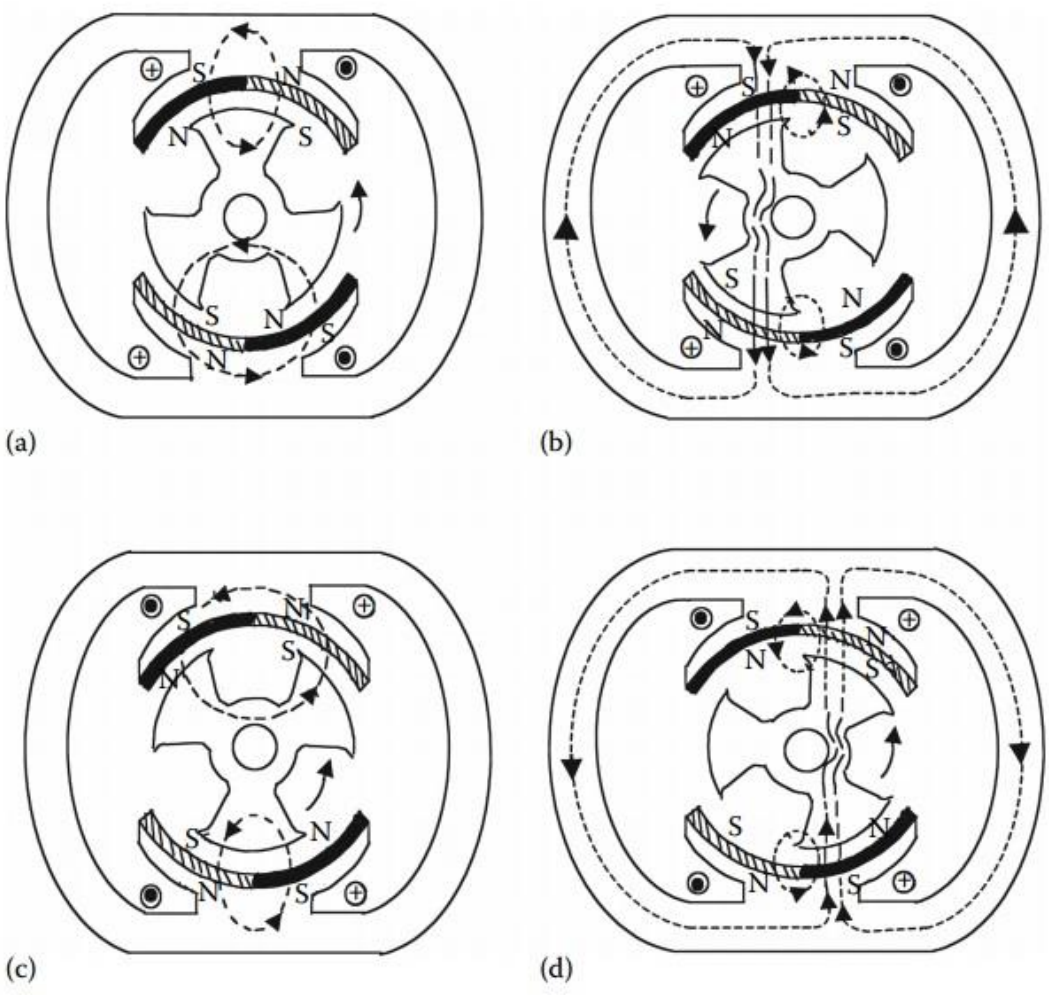

Figure 2.1 Illustration of FRM and its principle of operation. (a) Zero flux linkages position, (b) maximum positive flux linkages position, (c) zero flux linkages position, and (d) maximum negative flux linkages position.

2.2 Control operation

With stator flux linkage variation being alternating, the induced emf in the stator winding is also alternating and it may be considered to be a rectangular AC voltage assuming ideal linear variation of flux linkage [15]. When the stator winding is excited with the same polarity of the current as that of the induced emf, then the air gap power produced in the

machine is positive, resulting in motoring torque in either direction of rotation. When the stator winding is excited with the current that is of opposite polarity to the induced emf, then the machine is in regenerative mode with the machine supplying electrical power while taking the mechanical input power. Therefore, this machine with the appropriate power converter and control can operate in all the four quadrant operation.
Because the principle of operation is similar to that of the brushless DC motor (BLDCM), the FRM can be driven by alternating pulses [5] of rectangular current of 120° base and with a 120° shift between three phase of the stator. The pulse width modulation (PWM) pattern is commonly used in the two-phase feeding scheme to control the speed of the motor

The features of the FRMs are summarized in the following:
1. They have bidirectional flux with the outcome of ac machine characteristics. The flux linkages versus current have a four-quadrant characteristic as against one quadrant for the SRM.
2. PMs are on the stator and, therefore, these machines are easier to manufacture. Also the robustness of the rotor now makes it an ideal candidate for very high-speed operation unlike the machine with the PMs on the rotor.
3. The stator and rotor poles are salient and the punching of such laminations is simpler.
4. The coils are concentric, making them easier to manufacture and install in the machine.
5. The SRM superposed with PMs in its stator poles becomes a PM brushless dc machine in all its characteristics without the distributed windings, magnets on the rotor, and hence without much of a manufacturing cost.
6. Because of the PMs in the path of the flux, and as the relative permeability of the magnet is in the range of the air, the reluctance is very large, thus making the inductance of the winding very small, resulting in a small time constant of the winding. This leads to a fast torque response, a desirable feature in high-performance applications.
7. Core losses increase in this machine compared to the SRM due both to the sweeping PM flux in the rotor iron and the presence of bipolar flux in the machine laminations.
8. The PMs may experience the elevated temperature of the stator poles, which will reduce their residual flux density, thus reducing the output of the machine. Because of the PMs, the need for keeping the temperature rise to a certain safe value for the sake of PMs in the stator

poles will reduce the overall power output of the machine.

9. The harmonic torques will be fairly high in these machines and because of this fact they may not be suitable for high-performance servo applications.

CHAPTER 3

Design Procedure of Flux Reversal Machine

3.1 Basic configuration

A general rule regarding the stator and rotor number of poles N_S, N_r , and the number of phases *m* for the multiphase FRM is given by

$$\frac{N_S}{N_r} = \frac{m}{m+1} \tag{3.1}$$

Therefore, N_S/N_r = 3/ 4, 6/ 8, 12/ 16 are some candidates for a three-phase FRM.
From experience, we choose 6/ 8 configuration, as shown in Figure 3.1(a). The coil terminal connections are shown in Figure 3.1(b).

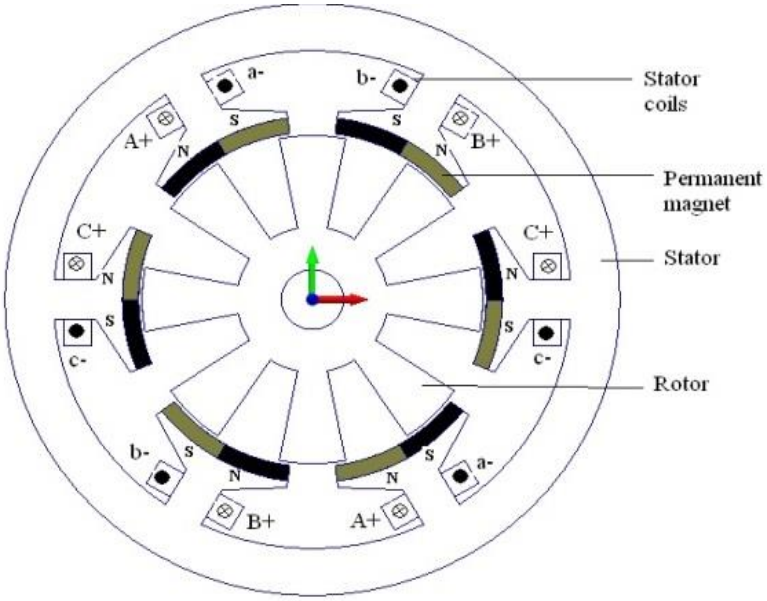

Figure 3.1a: Cross section of 6/8 FRM

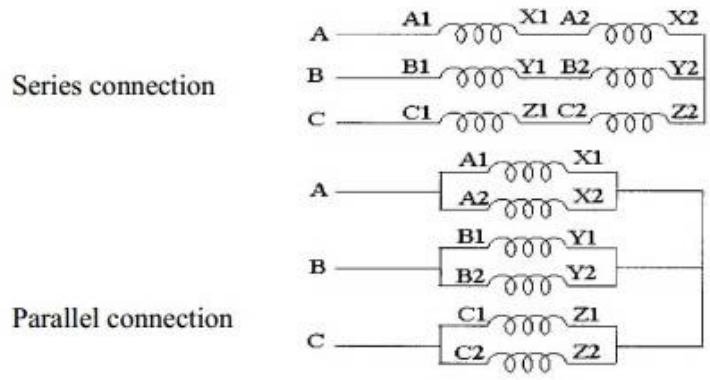

Figure 3.1b: Interconnection of stator coil.

3.2 Electromagnetic power at base speed

The procedure for sizing FRM based on their power requirement [16]. Assuming the machine will rotate at 1500rpm speed. This speed is considered as the base speed at which the torque is maximum. The efficiency ɳ at base speed is approximately 0.6 to 0.80.

The machine design for 1kW and 1500rpm. If the efficiency ɳ is 75% then the electromagnetic power P_e is

$$P_e = \frac{1000}{0.75} = 1333.33W \tag{3.2}$$

Specific electrical and magnetic loading determines the tangential force f_t. Relation between machine electromagnetic power and machine dimension is given by

$$P_e = f_t(\pi D_r l_{stk})\frac{D_r}{2}\Omega_r \tag{3.3}$$

Where D_r is Rotor Diameter.

l_{stk} is stack length of the machine.

Ω_r is the rotor speed in rad/sec.

The ratio between stack length and rotor diameter λ is define as

$$\lambda = \frac{l_{stk}}{D_r} = 0.2\text{- }1.5 \tag{3.4}$$

From equation 3.3 and 3.4, the rotor diameter is given by

$$D_r = \left(\frac{2\times P_e}{\pi f_t \lambda \Omega_r}\right)^{1/3} \quad (3.5)$$

We choose a tangential force density of $f_t = 1.3\times10^4$ N/m^2 and $\lambda = 1.2$ then from equation (3.5) yields

$$D_r = \left(\frac{2\times1333.33}{\pi\times1.3\times10^4\times1.2\times2\pi\times25}\right)^{1/3} = 0.0702\approx 0.07\text{m} \quad (3.6)$$

The Stack length is ,

$$l_{stk} = \lambda D_r = 1.2\times0.07 = 0.084\text{m} \quad (3.7)$$

Corresponding to the base electromagnetic power, the base electromagnetic torque is

$$T_e = \frac{P_e}{\Omega_r} = \frac{1333.33}{2\pi\times25} = 8.488\ \text{Nm} \quad (3.8)$$

3.3 PM Airgap Flux Density

The permanent magnet materials are ceramic, alnico, samarium cobalt and neodymium iron boron(NdFeB). In a permanent magnet machine with plastic bonded or ferrite magnets, the magnet losses are neglected, due to their very high resistivity. But in rare earth magnets(NdFeB), the resistivity is much lower. Therefore, it is very important to know those losses. Generally the eddy current losses are less in electrical machines, but they heat the rotor and may demagnetize the magnets if they are heated to a high temperature such as 120^c for NdFeB magnet. The PM ideal flux density at the surface of the PM (on the airgap side) B_{PMi} is the same as the airgap flux density B_{gi}. Also, with a linear demagnetization (B_m, H_c) curve for the PM, we have

$$B_b = \frac{B_r}{1+\frac{\mu_{re}}{\mu_0}[\frac{(1+k_{st})g}{h_m}]} = B_{gi} \quad (3.9)$$

where μ_{re} is the recoil permeability, $\mu_0 = 4\pi\times10^{-7}$ H/ m, the permeability of free space, h_m is the PM radial thickness, g is the airgap, and k_{st} is a global saturation factor.

To find the magnet thickness, we proceed as follows. First, to obtain a low inductance and hence a low time-constant, a thick magnet would be desirable.

However, a thick PM would imply a higher cost. We choose h_m=3mm and airgap, g = 0.5mm and Nd FeB 52 MGOe magnets are used.
The properties of this magnet are given in Table 3.1.

Table 3.1 The properties of NdFeB 52 MGOe Magnet

Residual flux density	B_{r0} = 1.48T
Coercive force	H_{c0} = 0.891 MA/m
Recoil Permeability	μ_{re} =1.29μ_0 H/m
Temperature coefficient for B_r	k_{Br} = -12%/^{0}C
Temperature coefficient for H_c	k_{Hc}= -65%/^{0}C

At an operating temperature of 25^{0}C, we have

$$B_r = B_{re}\,[1+\frac{k_{Br}}{100}(T-25)] = 1.382\ T \quad (3.10)$$

$$H_c = H_{c0}\,[1+\frac{k_{Hc}}{100}(T-25)] = 0.572\ MA/m \quad (3.11)$$

And the recoil permeability becomes

$$\mu_{re} = \frac{B_r}{H_c} = \frac{1.382}{0.572}.10^{-6} = 2.42\times10^{-6} = 1.92\mu_0 \quad (3.12)$$

Finally from equation (3.9), we obtain

$$B_{gi} = \frac{1.382}{1+\frac{1.92\mu_0}{\mu_0}[\frac{(1+0.05)0.5}{3}]} = 1.034\ T \quad (3.13)$$

The PM flax per stator pole ϕ_{PM} is

$$\phi_{PM} = l_{stk}.B_{PMi}.\tau_{PM}.K_{fr} \quad (3.14)$$

Where, K_{fr}= Ratio between flux linking the stator winding to airgap flux.

τ_{PM} = Permanent Magnet pole arc length.

Which is given by,

$$\tau_{PM} = \frac{\pi D_r}{2N_r} = \frac{\pi \times 70}{2 \times 8} = 13.744 \text{ mm} \quad (3.15)$$

The stator flux linkage variation is almost sinusoidal with rotor position θ_r.

$$\phi_{PM}(\theta_r) = \phi_{PM}.\sin(N_r\theta_r) \quad (3.16)$$

Therefore, The PM flux per stator pole derivative with θ_r

$$\frac{d\phi_{PM}(\theta_r)}{d\theta_r} = l_{stk}.B_{PMi}.\tau_{PM}.K_{fr}.N_r.\cos(N_r\theta_r) \quad (3.17)$$

$$= l_{stk}.B_{PMi}.K_{fr}.\frac{\pi D_r}{2}.\cos(N_r\theta_r) \quad (3.18)$$

3.4 MMF per Coil at 1500 rpm

There are $\frac{N_s}{3}$ stator pole per phase and $\frac{N_s}{3}$ coils in series with n_c turns per coil . The EMF amplitude, E_m per phase is

$$E_m = \frac{N_s}{3}.n_c.2\pi n.l_{stk}.B_{PMi}.K_{fr}.\frac{\pi D_r}{2} \quad (3.19)$$

Where, n= Rotor speed in rotation per second.

The electromagnetic torque, T_e produce by I_q current control is given by,

$$T_e = \frac{3}{2}.E_m.I.\frac{\sqrt{2}}{2\pi n} \quad (3.20)$$

We calculate, $n_c.I = n_c.\frac{\sqrt{2}}{3}.T_e.\frac{2\pi n}{E_m}$ (3.21)

From equation (3.19), (3.20) and (3.21), we obtain

$$n_c.I = \frac{\sqrt{2}}{3}.T_e.\frac{1}{\frac{N_S}{3}.l_{stk}.B_{PMi}.K_{fringe}.\frac{\pi D_r}{2}} = 475.65 \text{ At/coil} \qquad (3.22)$$

3.5 Stator Slot Geometry

Stator slot/ pole geometry is shown in Figure 3. The slots are semi closed with a slot opening $w_{so} = 2\tau_{pm}/3$.

To calculate the slot area, we first determine the slot fill factor. Because space is required for axial air circulation, we choose a low fill factor $k_{fill} = 0.38$. To choose the core flux density, generator design would be different from motor design owing to the mode of cooling in the two cases. Finally, the choice of current density is a matter of compromise. A high current density reduces the machine size and machine time constant, but also decreases the machine efficiency. Low time constant improves the commutation process. Furthermore, at high speeds such as 18,000 rpm (or 2.4 kHz), skin effect is not negligible and results in a significant increase in copper losses. We have two choices here: either we use stranded wire or increase the slot area, hence the stator diameter and the machine mass. Litz wire may be appropriate for the motor primarily operating in extreme high speed. We choose the base current density

$$J_{cb} = 6 \text{ A/ mm}^2 \qquad (3.23)$$

The required slot area for the winding is obtained by choosing the current density(J_{cb}) and slot fill factor(K_{fill}). The slot area A_{slot} Is given by

$$A_{slot} = \frac{2n_cI}{J_{cn}.K_{fill}} = \frac{2\times475.65}{0.38\times6} = 417.24 \text{ mm}^2 \qquad (3.24)$$

The stator pole pitch τ_{sp} is given by

$$\tau_{sp} = \frac{\pi}{16}(D_r+2g) = \frac{\pi}{16}(71) = 13.94 \text{ mm} \qquad (3.25)$$

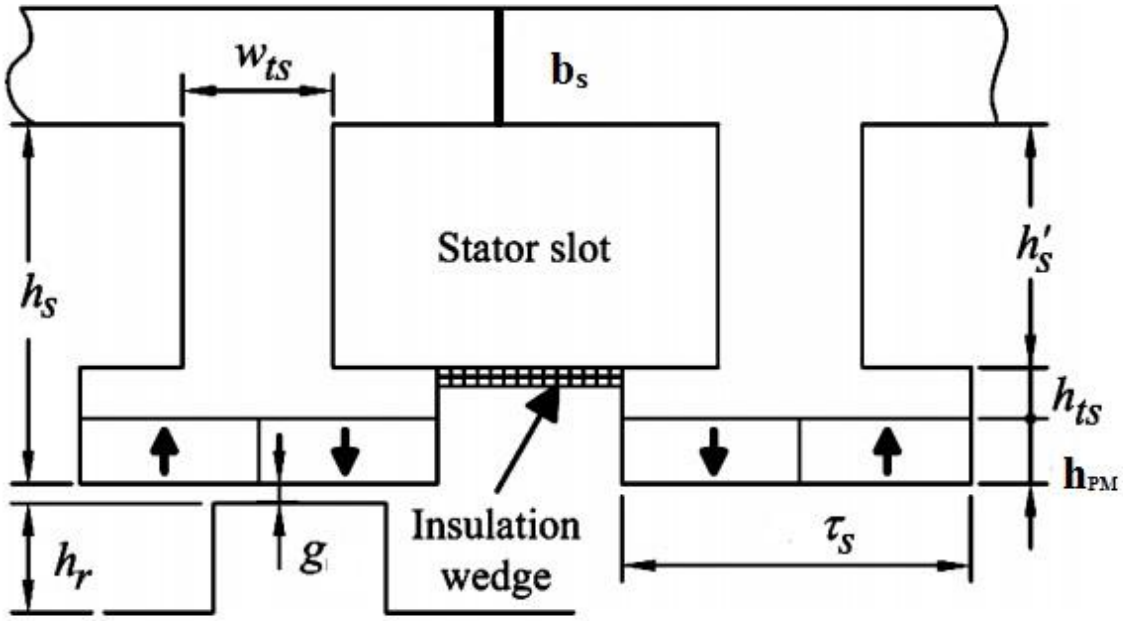

***Figure 3.2**: Stator slot geometry of Flux Reversal Machine.*

The precise geometry of a slot is shown in Figure 3.3.

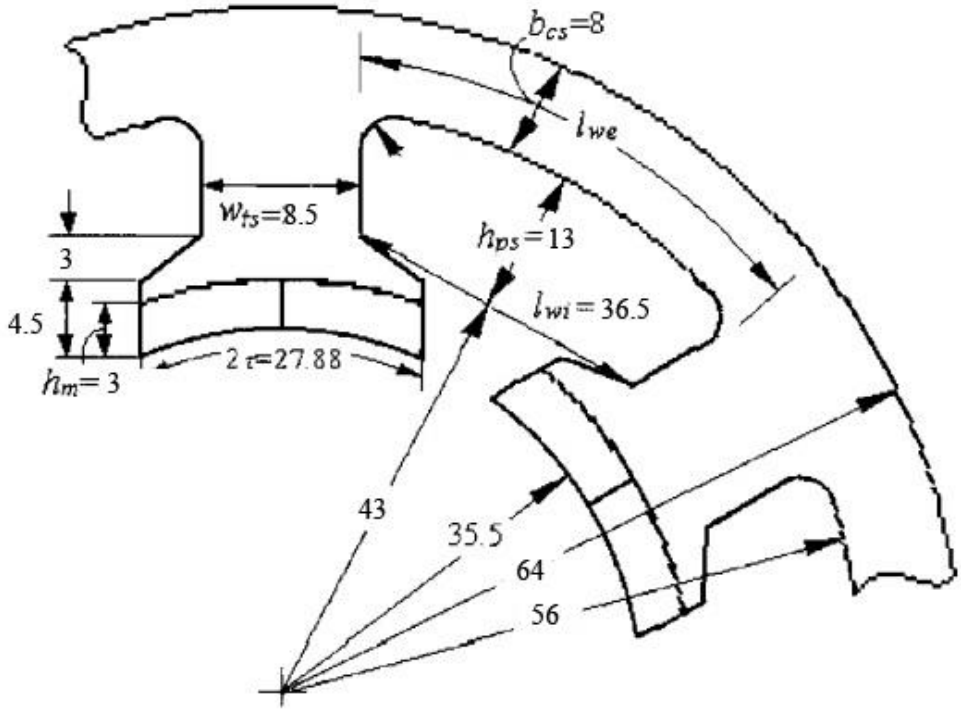

Figure 3.3: Refined slot geometry.

The maximum flux per pole is given by

$$\lambda_{PMmax} = \frac{1}{2}(1+k_{fr})l_{stk}\,\tau_{sp}\,B_{PMi} = \frac{1}{2}(1+0.44)\,l_{stk}\,\tau_{sp}.1.038 = 0.747\,l_{stk}\,\tau_{sp} \quad (3.26)$$

Choosing a pole flux density B_{ps} = 1.2T , the pole with w_{ts} is given by

$$w_{ts} = \frac{\lambda_{PMmax}}{l_{stk}B_{ps}} = \frac{0.747 l_{stk}\tau_{ps}}{l_{stk}\times 1.2} = 0.623\,\tau_{sp} = 8.68 \approx 8.5\text{mm} \quad (3.27)$$

the slot opening l_{wi} is given by

$$l_{wi} = \frac{\pi\times 86}{6} - w_{ts} = 36.5\text{mm} \quad (3.28)$$

Because A_{slot} = 417.24 mm^2, from equation (3.24), the useful slot height h_{ps} becomes 13 mm. Finally, the external pole diameter is given by

$$D_{pe} = 43+2h_{ps} = 86+26 = 112\text{mm} \quad (3.29)$$

The stator back-iron thickness is obtain from

$$b_{cs} = \frac{k_{fr}B_{PMi}\tau_{ps}}{2B_{cs}} = \frac{0.44\times 1.034\times 13.94}{2\times 0.5} = 6.34 \approx 8\text{mm} \quad (3.30)$$

Consequently the stator external diameter D_{se} becomes

$$D_{se} = D_{pe} + 2b_{cs} = 112 + 2\times 8 = 128\text{mm} \quad (3.31)$$

3.6 Rotor Core Geometry

The rotor core geometry is shown in Figure 3.4. For the purpose of reducing windage loss, the interpole areas should be filled with lightweight nonmagnetic material.

The rotor has 8 poles and 8 interpoles. The motor back core is designated by b_{cr} and the shaft by D_{sh}. The angles subtended by the pole α and by interpoles β are such that $\alpha = \beta = \frac{\pi}{8} = 22.5°$. The interpolar space is rounded off near the back iron to reduce fringing.

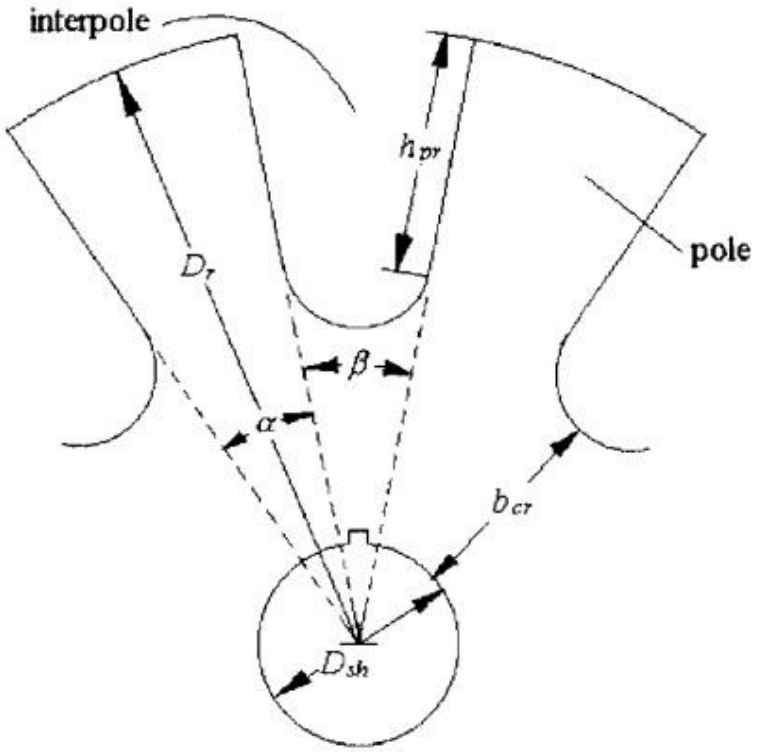

Figure 3.4: *Rotor core geometry.*

For mechanical integrity, we estimated that

$$D_{sh} = 20mm \tag{3.32}$$

Also, we assume that the rotor back-iron thickness b_{cr} could be made same as that of the stator b_{cs}. Thus

$$b_{cr} = b_{cs} = 8mm \tag{3.33}$$

and the pole height h_{pr} becomes

$$h_{pr} = \frac{1}{2}(D_r - D_{sh} - 2b_{cr}) = \frac{1}{2}(70 - 20 - 16) = 17mm \tag{3.34}$$

Following data is assumed for design the machine.

- the tangential force $f_t = 1.2$ N/mm^2
- $\lambda = 1.2$
- Efficiency of machine $\eta = 75\%$
- Flux leakage factor $K_{fri} = 0.45$
- Slot fill factor $K_{fill} = 0.38$
- Winding current factor $J_{cn} = 6$ A/mm^2

Table 3.2 shows the dimensions of 6/8 pole FRM

Sr. No	Description	Symbol	Value
1	Number of stator pole	N_s	6
2	Number of rotor pole	N_r	8
4	Air gap	G	0.5 mm
5	PM height	h_{PM}	3mm
6	Rotor pole span angle	α_r	22.5°
7	Stator pole span angle	α_s	45°
8	Stator pole height	h_s	20.5mm
9	Rotor pole height	h_r	18mm
10	Outer diameter of Rotor	D_r	70mm
11	Outer diameter of Stator	D_s	128mm
12	Stack length of machine	l_{stk}	84mm

Table 3.3: Materials of FRM

Type	Material
Magnet	NdFeB
Stator	M19 steel
Rotor	M19 steel

CHAPTER 4

FINITE ELEMENT ANALYSIS

4.1 FINITE ELEMENT ANALYSIS [17]

The fundamental physical equations that describe the electromagnetic fields are given by Maxwell's equations as

$$\nabla . B = 0 \quad (4.1)$$

$$\nabla \times E = -\, dB/dt \quad (4.2)$$

$$\nabla \times H = J \quad (4.3)$$

Equations (4.1)-(4.3) are presented in terms of vector field variables E, B and H, but these equations are usually solved by using vector potential formulation.

The magnetic vector field B can be written in term of the vector potential as:

$$B = \nabla \times A \quad (4.4)$$

Also, the relationship between H and B is expressed as follow:

$$H = \mu . B \quad (4.5)$$

Vector potential equation for magnetic field is obtained by substituting equations (4.4) and (4.5) in equation (4.4), yields

$$\nabla \times (\mu . \nabla \times A) = J \quad (4.6)$$

To numerically solve equation (4.6), the finite element method is used. In this paper, the open source software FEMM version 4.2 is employed. This software is able to solve two-dimensional partial differential equations.

4.2 FEMM modeling though LUA script

The FEMM also supports LUA scripting language. The LUA scripted library can be used to draw the layout of the FRM motor in FEMM through the process of drawing as shown in Fig.4.1. All motor parameters can also be specified in the LUA script. After modeling, meshing of finite elements will solve problem differential equation in modeling of FRM motor. The meshing yields

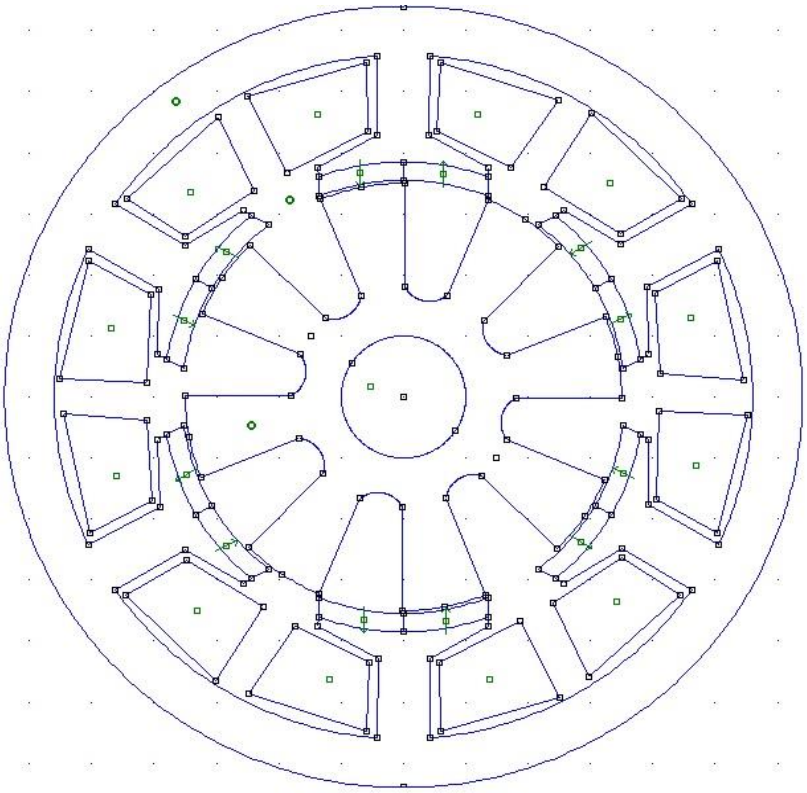

Figure 4.1: *Modeling 6/8 pole FRM by FEMM.*

approximately 21,000 nodes and 50,000 elements. To improve the accuracy of cogging torque calculations, the meshing around the arcs and corners has to be higher resolution as shown in Figure 4.2. It is a well-known fact that

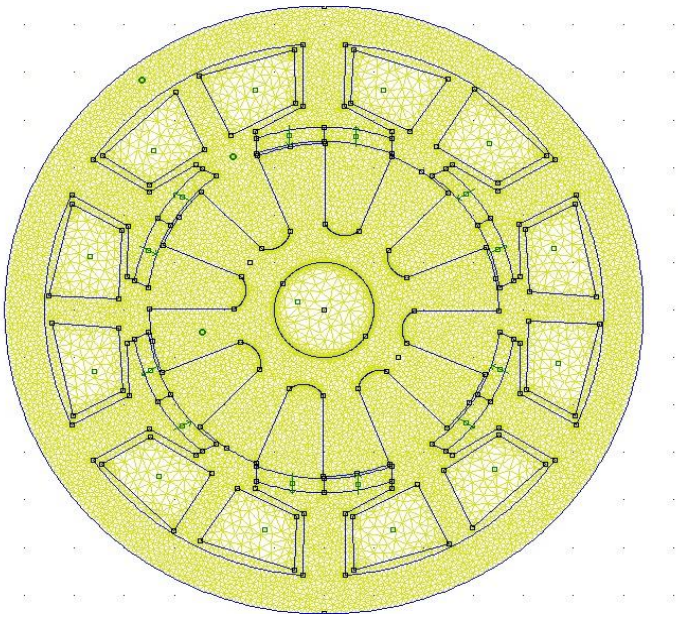

***Figure 4.2**: FEEM mash of FRM*

by increasing the meshing resolution, a higher accuracy in estimation can be reached but only to a certain extent. Where by the increase of meshing nodes of 20,000 to 140,000 produces an increase in accuracy of approximately 0.2%.

4.3 Simulation steps

In the simulation, the model can be drawn in FEMM software or imported as an AutoCAD file. The material and mechanical properties are specified by setting the LUA script. The domain is meshed and the boundary conditions are determined by user. The software uses a triangular element to mesh the domain and linear functions to approximate the solution. There are approximately 21,000 nodes for entire FRM motor model. After setting the meshing, the cogging torque for the initial rotor position is calculated by using the weighted stress tensor method. A flowchart of FEMM simulation is provided in Fig.4.3. The meshing process and cogging torque calculation are performed before the rotor position is

increased by a certain degree. These processes are repeated and results are recorded at each incremental rotor position until the final rotor position is reached. In this paper, the FEMM simulation is finished at 45 degree.

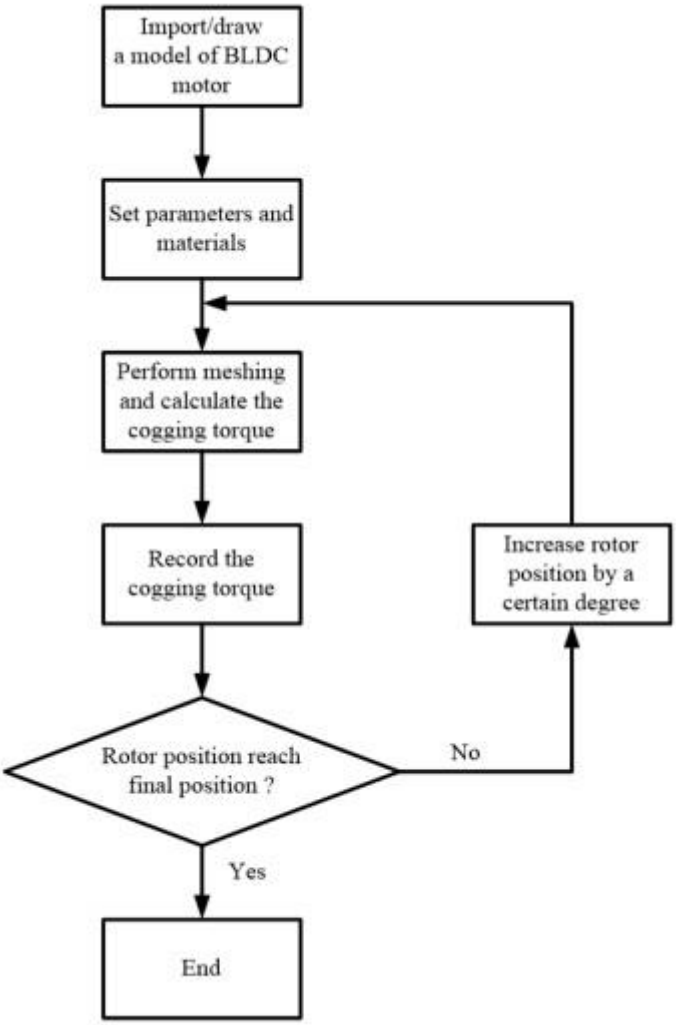

***Figure 4.3**: Simulation steps on cogging torque calculation.*

CHAPTER 5

SIMULATION RESULTS

5.1 Conventional 6/8 FRM:

The three phase 6/8 pole FRM is shown in fig.3.1A. Its specifications and materials are given in Tables 3.2 and 3.3, respectively. Flux distribution in the machine at no load is shown in Fig. 5.1

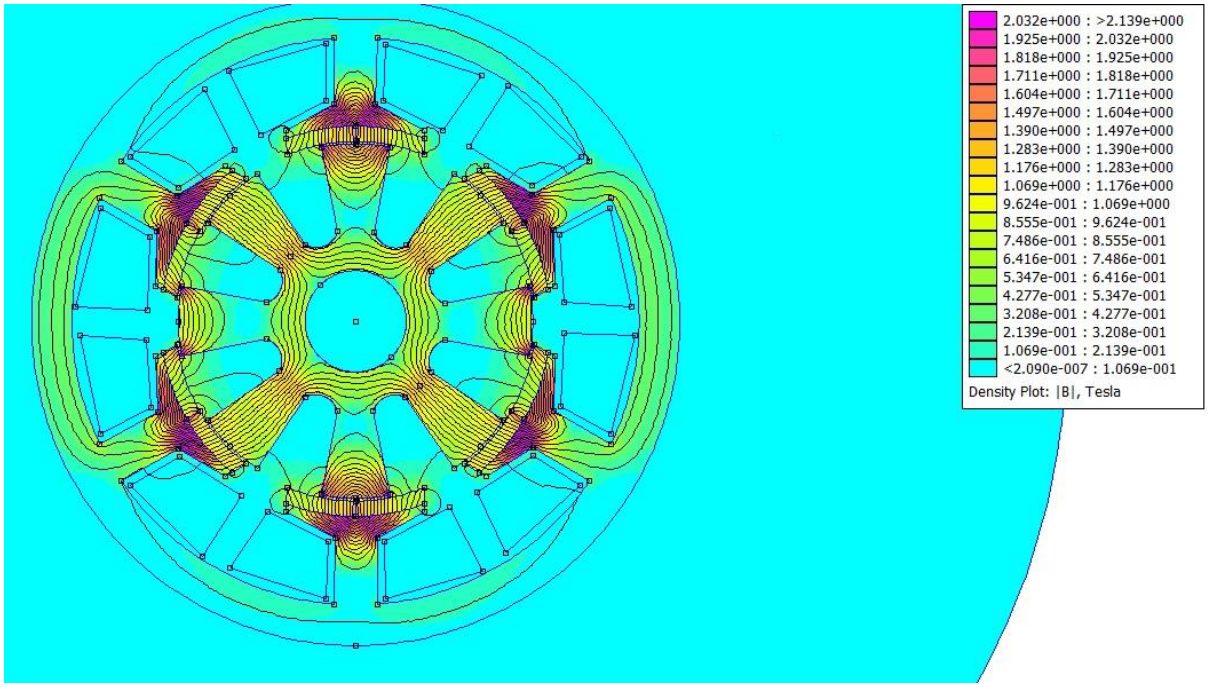

***Figure 5.1** : Flux distribution of 6/8 FRM*

Cogging torque of electrical motor is the torque due to the interaction between the permanent magnet of the stator and the rotor slot of a Permanent Magnet machine. It is also known as detent or no current torque. FRM consists of permanent magnet on the stator teeth and this fundamentally causes problems related to cogging torque. The cogging torque of the FRM causes noise, vibration and exerts a bad influence upon position sensing.

The cogging torque of this machine obtain from simulation shown in figure 5 The cogging torque repeats itself every 15 mechanical degrees and is anti-symmetric with relevance to **θ** = 7.5 mech. degree due to the flux reversal. The periodicity can be explained using an approach analogous to that used for brushless DC motors . The airgap permeance variation with rotor position has a cycle of $\mathbf{2\pi/N_r}$, whereas the PM MMF has a cycle of $2\pi/N_s$. It may then be intuitively inferred that the cogging torque cycle is $2\pi/S$, where *S* is the least common multiple of $\mathbf{N_s}$, and N_r.. For the case in point, $N_s = 6$ and $N_r = \mathbf{8}$, and thus $S = 24$, so the cogging torque cycle is 360/24 = 15 mech. Deg., which agrees with the FEA results (Fig. 5.2).

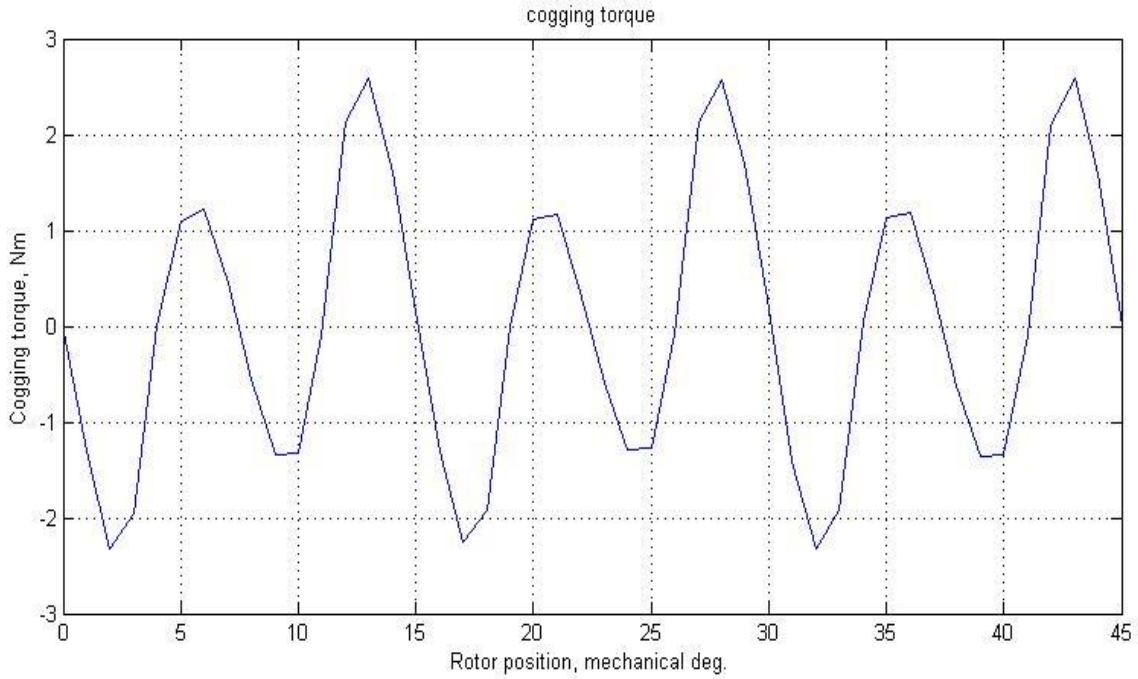

Figure 5.2 : cogging torque

The back EMF of the machine at no load condition at 1500 rpm shows in figure 5.3

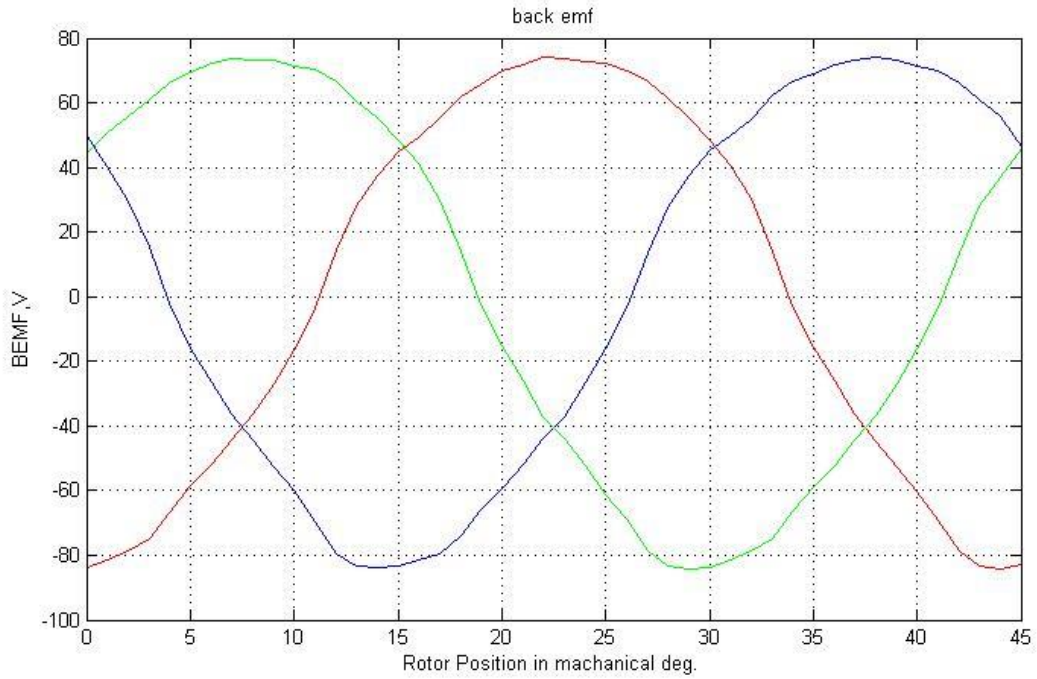

Figure 5.3 : BEMF wave form at 1500 rpm.

5.2 Inset type FRM

This is a new FRM has permanent magnets parallels to the stator magnet flux lines and these are much more difficult to demagnetize [18]. This new design is effective in decreasing the flux leakage and cogging torque. Fig. 5.4 compares the inset type FRM with a conventional FRM.

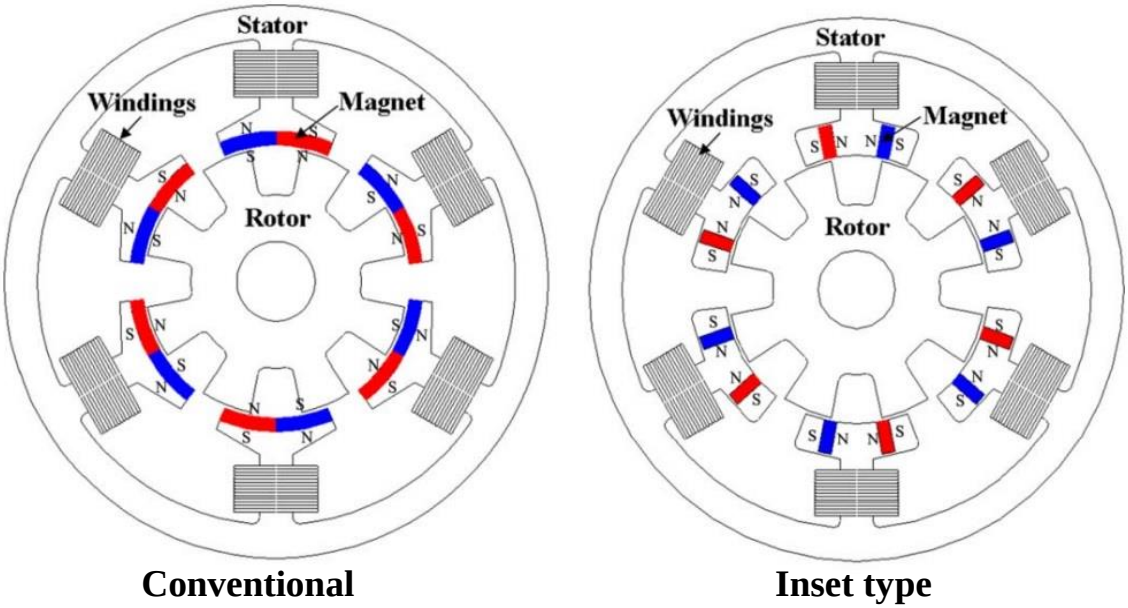

Figure 5.4: The conventional and inset type FRM

The inset type FRM is designed to have the same specification of conventional FRM except the amount of permanent magnet. To get same torque ability as conventional FRM, we choose magnet thickness h_m, 2.5mm and height is 5.5mm for inset type FRM after many FEM calculation with thinner and thicker and various heights of PM. Fig 5.5 show the flux distribution of inset type FRM.

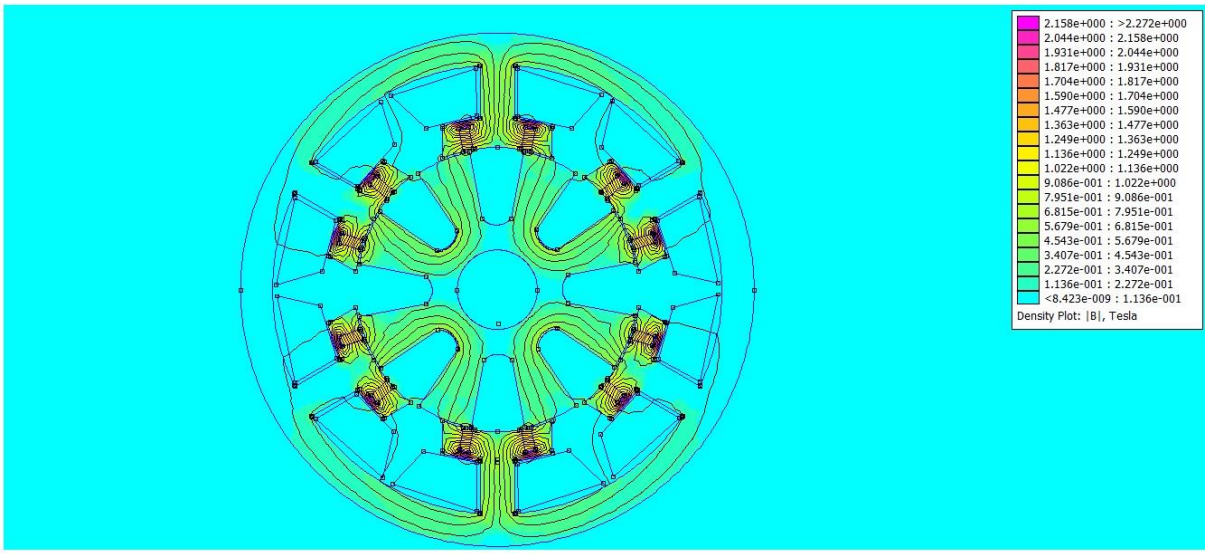

***Figure 5.5**: Flux distribution of Inset type FRM*

5.3 FEM Analysis result for Inset type FRM

5.3.1 Cogging Torque :

Figure 5.6 Shows the cogging torque of inset type FRM which is much lower than conventional FRM. The cogging torque also repeats every 15 mechanical degree as expected.

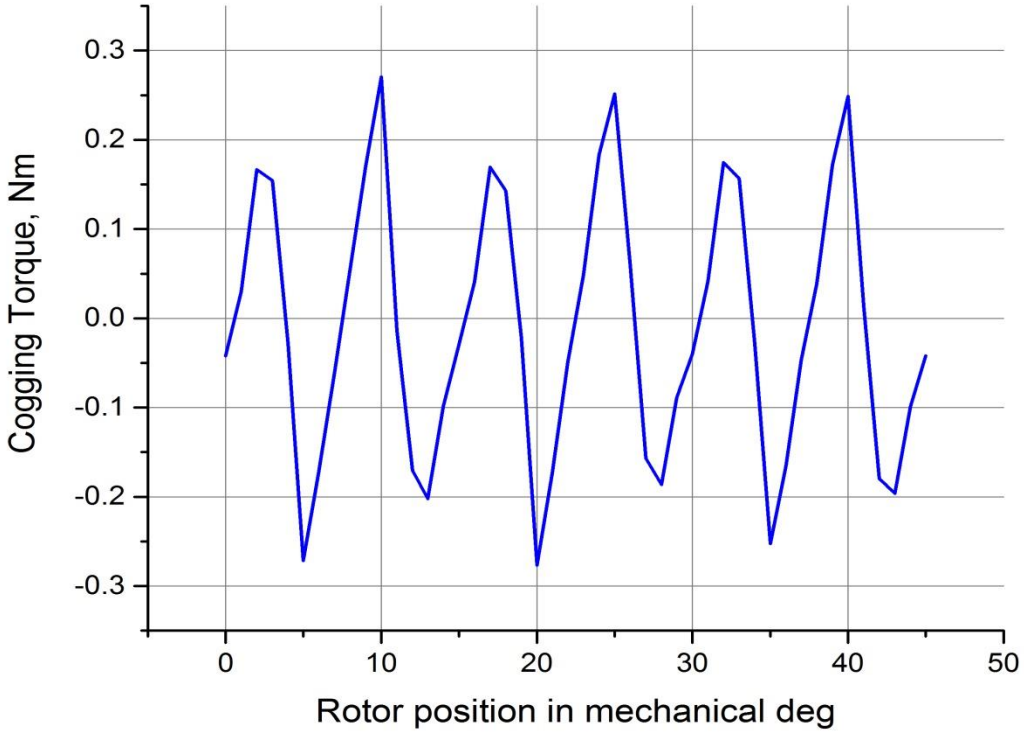

***Figure 5.6** : Cogging torque*

5.3.2 Back EMF

Torque and back electromotive force (BEMF) constant of an FRM are the same, so we can know the torque ability from the BEMF waveform. Fig. 5.7 compares the BEMF of the conventional and inset type FRM at 1500 r/min. There is no difference in the generated BEMF although the amount of the permanent magnet used in inset type FRM is about 33% compared to the conventional one. This is because the flux leakage in the air gap is reduced and the magnetic circuit becomes effective.

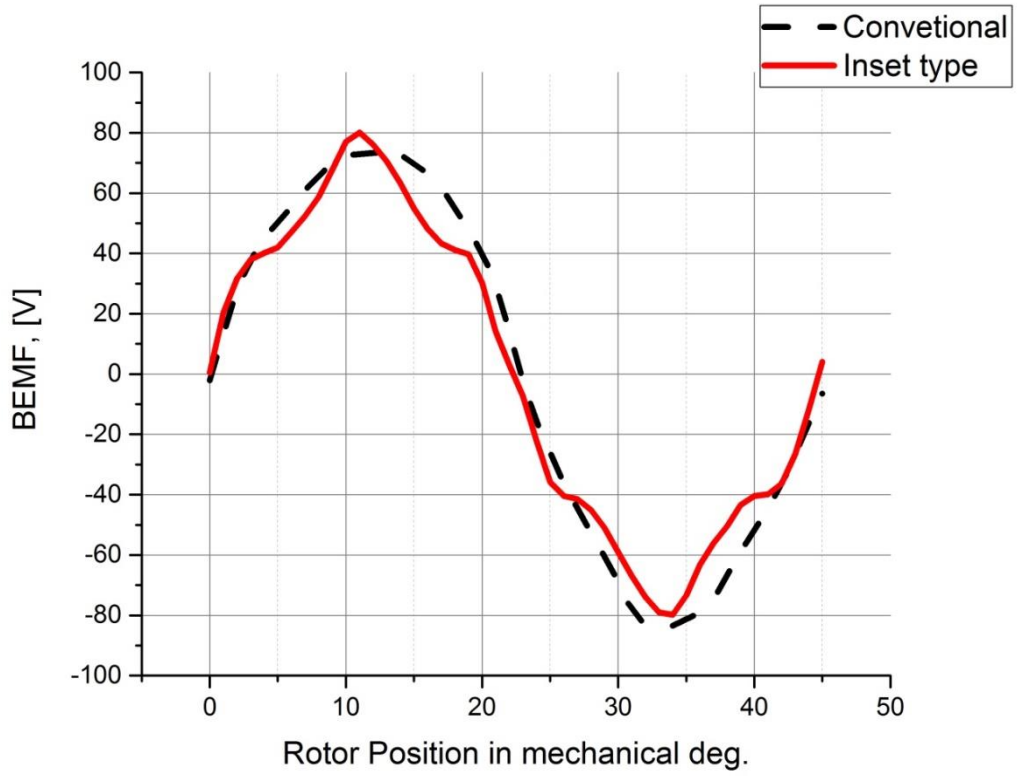

Figure 5.7 : BEMF at 1500 rpm

5.3.3 Static performance of Inset type FRM

We may simulate steady state condition by applying different current in phase A.

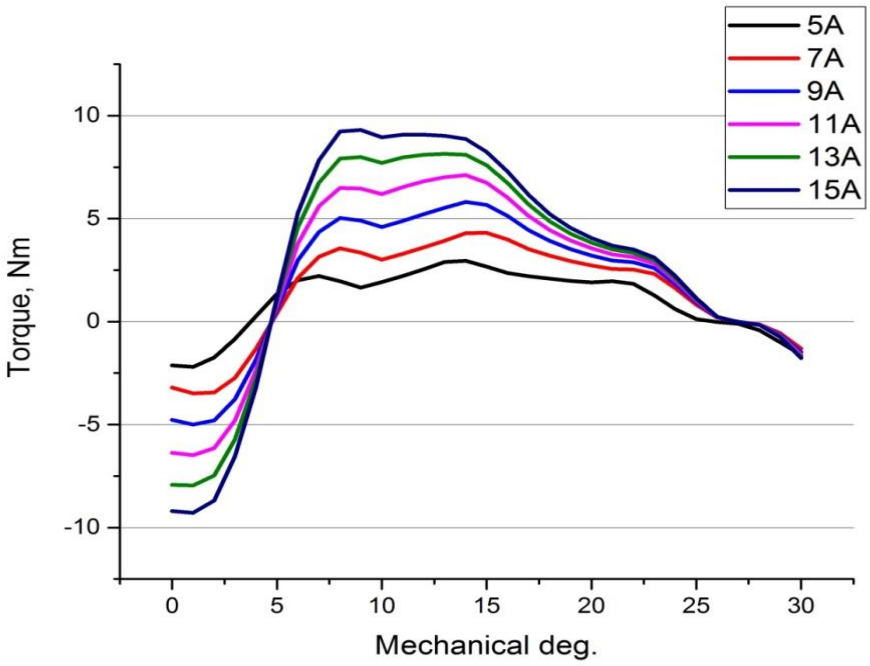

***Figure 5.8**: Interaction torque at phase A with different current.*

5.4 Influence of design parameter on torque

Now we investigate the effect of various design parameters on torque. In order to simplify the investigation and also to highlight the influence of each individual design parameter on the torque, it is assumed that all other design parameters remain unchanged while one design parameter is varied. Also we only look into the effect on peak torque when 9A current apply on phase A.

5.4.1 Stator Back iron thickness

Fig.5.9 shows the impact of stator back iron thickness on peak torque. Here the stator back iron thickness is express in terms of rotor pole length τ_{PM}. We can see that highest peak found when stator back iron thickness is 60% of $\tau_{PM.}$

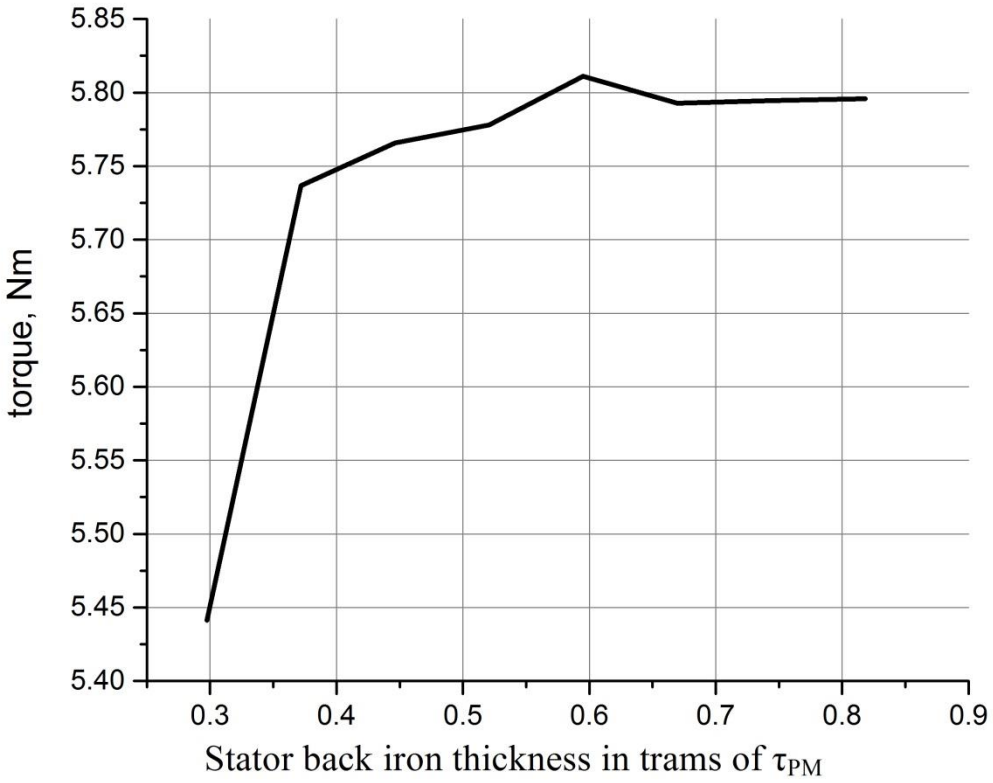

Figure 5.9: Peak torque variation at different stator back iron thickness.

5.4.2 Stator Pole Width

Figure 5.10 shows the effect of change of stator teeth width on torque when phase A is excited with 9A current. When stator teeth width is decreasing slot area is increasing hence flux-linkage and torque reduced.

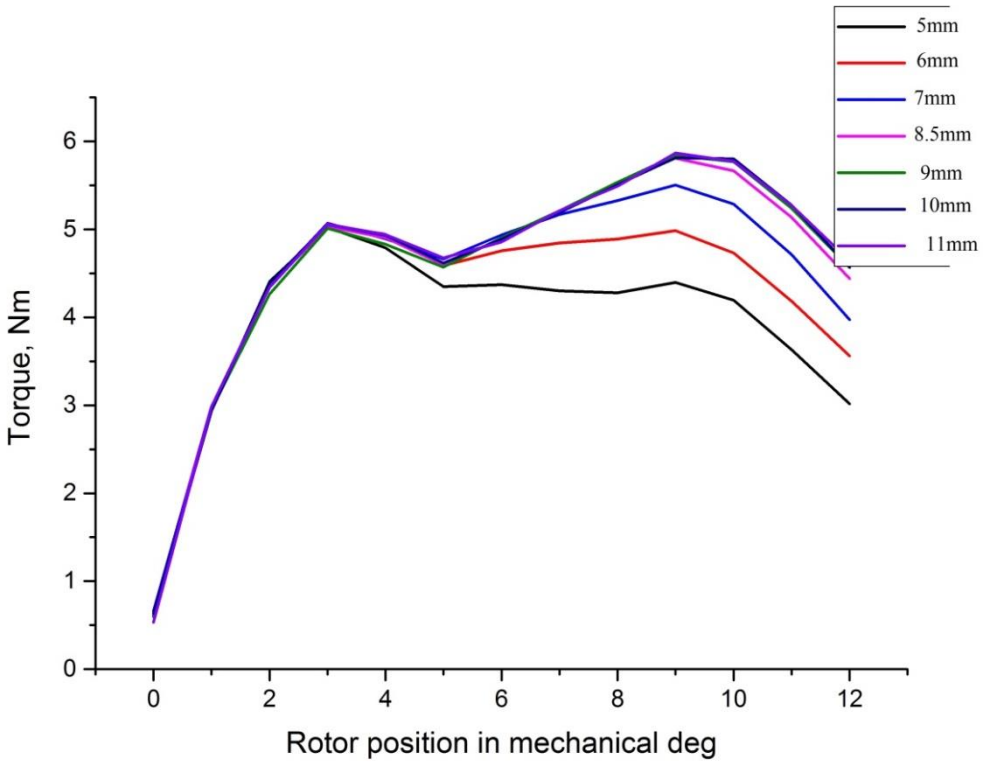

Figure 5.10 : Interaction torque in phase A at different stator pole width

Figure 5.11 shows the peak to occur when stator teeth width is $0.65\tau_{PM}$.

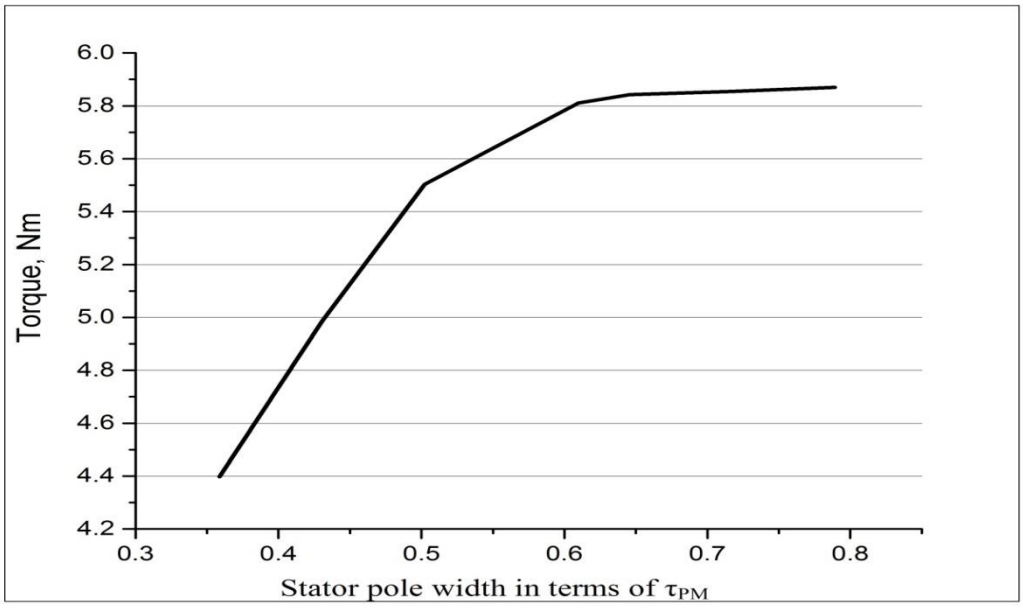

Figure 5.10 : Interaction torque in phase A at different stator pole width

5.4.3 Rotor Back iron thickness

Fig. 5.12 shows the impact of rotor back iron thickness on peak torque. Here the Rotor back iron thickness is express in terms of rotor pole length τ_{PM}. We can see that highest peak found when stator back iron thickness is 67% of τ_{PM}

.

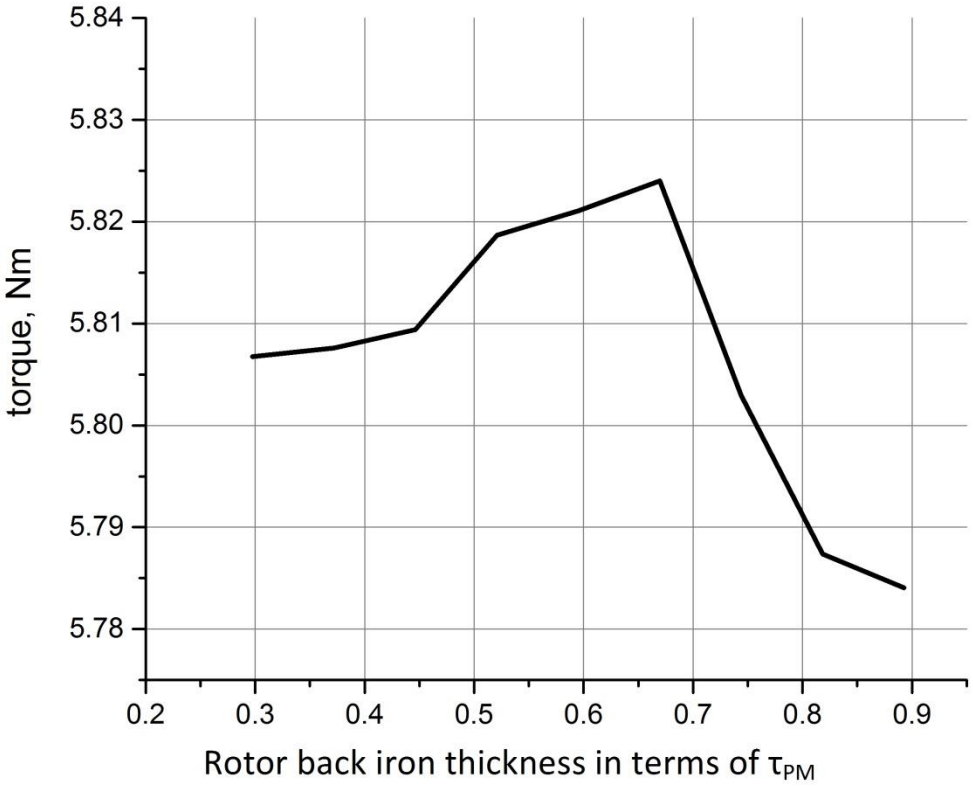

Figure 5.12 : Peak torque variation at different rotor back iron thickness

5.4.4 Rotor Pole Arc:

Figure 5.13 shows the cogging torque profile of the motor for various rotor pole arcs, from which it is observed that the change in rotor pole arc changes the magnitude of the cogging torque. It is also observed that for the rotor pole arc of 18° and 24° the peak of the cogging torque is the highest, while for the rotor pole arc of 20 to 22.5° the cogging torque is minimum.

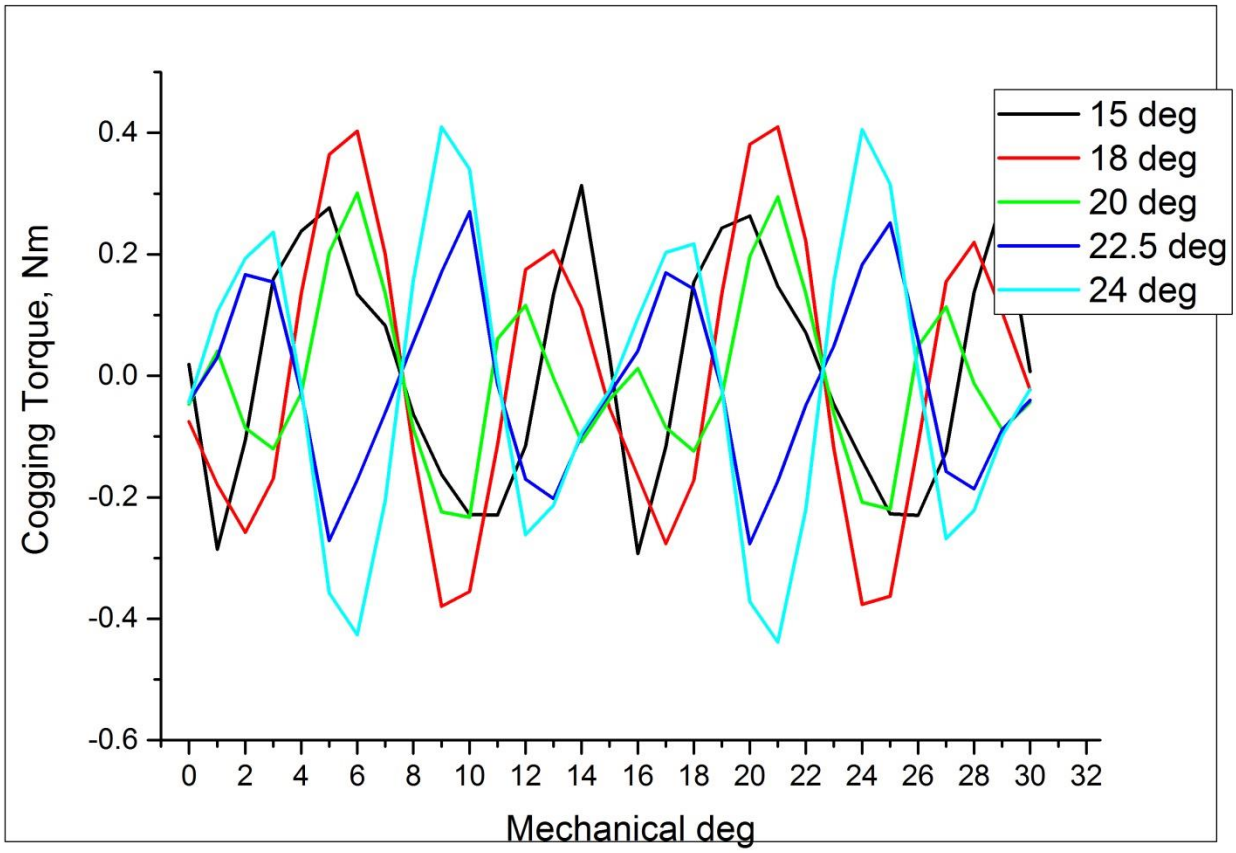

Figure 5.13: *Cogging torque for different rotor pole arcs.*

The effect of rotor pole arc variation on inset type FRM is not same as conventional FRM. In the conventional FRM the change in rotor pole arc not only changes the magnitude of the cogging torque but also the cogging torque frequency and for the rotor pole arc of 15° the

peak of the cogging torque is the highest, while for the rotor pole arc of 22.5° to 24° the cogging torque is minimum.

Figure 5.14 shows the effect of change of rotor pole arc on torque when phase A is excited with 9A current. For the rotor pole arc of 22.5° and 24° the torque ripple is high.

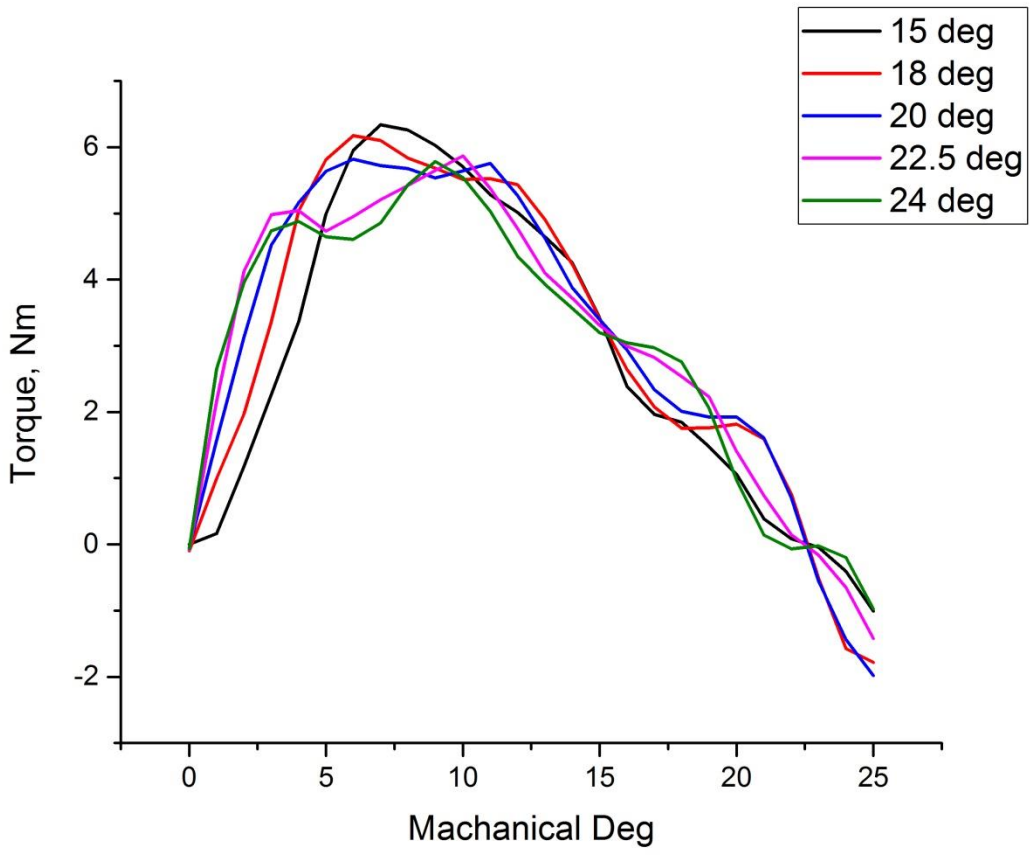

Figure 5.14: *Interaction torque in phase A at different stator pole arc.*

5.4.5 Rotor pole height

In general, the reluctance torque is negligible in a FSPM machine. However, the electromagnetic torque in FSPM machine, which is produced by the permanent magnet excitation torque, relies on the rotor saliency. Figure 5.15 shows that as the radial height of the rotor tooth is increased, the torque increases. Further increasing the radial height of the rotor tooth reduces the torque, due to the increase in the magnetic potential drop in the rotor tooth body due to magnetic saturation and an increase in flux leakage.

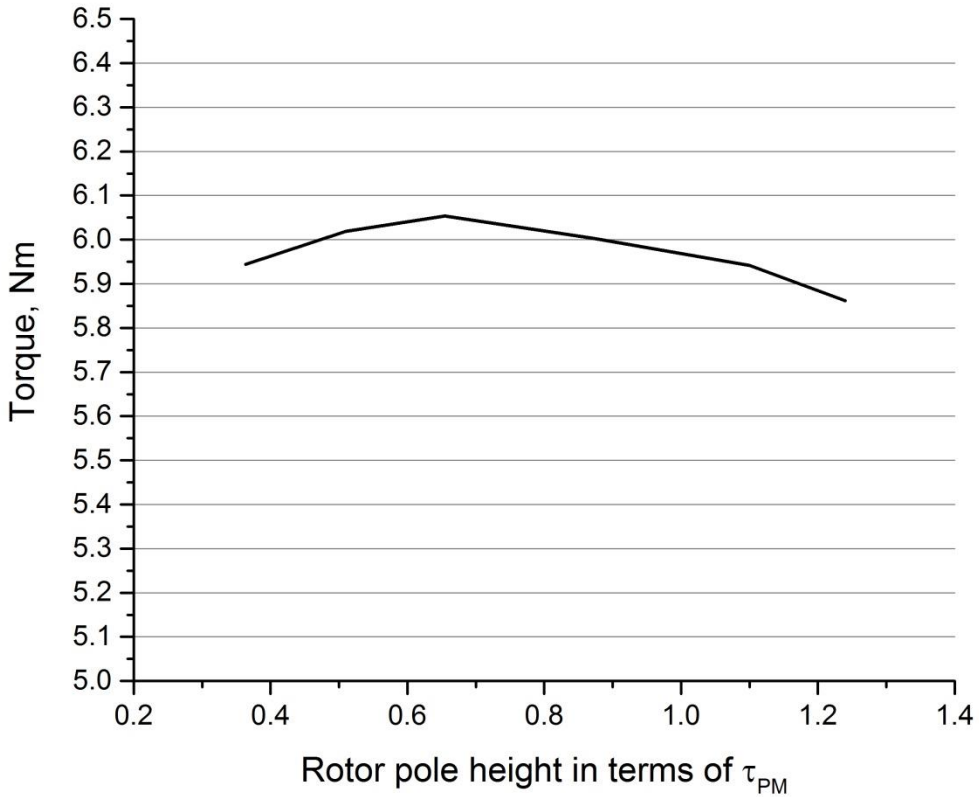

Figure 5.15: *Peak torque variation at different rotor pole height.*

CAPTER 6

Application of FRM

6.1 Low speed applications

Low-speed electric drives are being used in numerous industrial applications such as food-processing industries, precision positioning to low- weight ship propulsion and wind power generation. By low speed it means that machines which operates at a speed less than 150 r/min and torques of tens and hundreds of Newton meters. Low speed drive applications have been handled through indirect electric drives, because travelling- field winding stator cannot be actioned efficiently at such a speed as the pole pitch tends to be below 30mm.
The performance of high-energy permanent magnets allowed recently to look for direct drives for low speeds. The main benefits from direct drives (i.e. Eliminating mechanical gear) are

- Reduce the plant engineering and installation cost.
- Better position accuracy as the backlash is absent.
- Lower maintenance cost.
- Higher overall efficiency.

The first FRM for low-speed servo drive application is presented in [19].This machine had 28 rotor poles and 12 stator poles with 2 PM pairs on each stator pole. This machine is designed for128 r/min at 60Hz [20]. High torque density with less than 3% torque pulsation was achieved by vector control.

The two stator flux reversal machine was designed to achieve good torque density at efficiency of more than 0.9, power factor above 0.75 with a peak torque of 150Nm and 130rpm speed. For sinusoidal current control 3% torque pulsation was achieved [21].

6.1.1 Rooftop wind power generation

The rooftop-wind turbines have the potential to provide electricity to domestic and commercial applications. These generators can be directly driven, thus, eliminating the gearbox. Low acoustic noise is one of the requirements of rooftop-wind generation system. This can be achieved by reducing the cogging torque with skewing of the rotor. Depending upon the output power, the variation in the rated speed of the rooftop-wind turbine is 140 to 500r/min with 1-5kw range of generating capacity. The speed and power range require a large number of poles and stator slots in existing machines such as permanent magnet synchronous machine (PMSM) and induction machines, resulting in large air-gap diameter. However, FRM can have a large number of poles with less stator slots. This low speed machine can be directly connected to wind turbine eliminating the gearbox, thus, reducing the maintenance as well as the weight of the tower. Hence, FRM is best suited for direct-driven-rooftop wind power generation [22].

6.1.2 Voltage regulation

One of the limitations of permanent magnet generator is that it has high voltage regulation, as the magnet field cannot be controlled [23]. The recent work on FRM has shown the machine to be suitable for wind energy conversion, but it has very poor voltage regulation due to high armature reaction. Capacitors were connected in series to compensate for this armature reaction. The rating of capacitor banks equal to the machine rating it increases costs and reduces reliability. In case when generator output is connected to power electronic converter, the reactive power must be supplied by the converter. This increases rating of the converter. A flux switching machine with full pitch

winding has better flat voltage regulation characteristics than FRM. FSM has an edge over FRM [24].

6.2 High speed applications

High speed generators have numerous applications. The reason for this is that with modern manufacturing process with low tolerances, it is possible to manufacture high-speed electrical machines at low cost. For high speed generator, the rotor speed is normally above 100,000 RPM and the frequency of flux variation in the stator and rotor cores can be more than 1 kHz [25]. The flux reversal machine is appropriate for high-speed applications because of suitable structure [26] [27]. The first single phase FRM was introduced in [12] for automobile applications to replace the claw pole alternator because of the technical problems such as the mechanical stress caused by the centrifugal forces at high speeds and low efficiency mainly caused by eddy current losses.

The three-phase FRM for an automotive generator was proposed in [28] to measure the various losses and segregate the core loss extensive tests were carried out. When the FRM is coupled with the induction motor, the load on the motor changes. The total losses of the induction motor under this condition may be obtained by referring the terminal voltage to the P-V2 relationship. By repeating the procedure for each frequency, the total losses of the induction motor when coupled to the FRM are obtained. Thus, the total loss of the FRM can be calculated by subtracting the total induction motor losses and the resistive loss from the total input power.

Two-phase two stator 4/2 pole Flux reversal PM alternator was presented in [29]. Due to the low number of poles, this structure is suitable for high-speed application. With a proper control, the FRM can operate as a high speed motor with wide speed range and better torque performance [30].

CHAPTER 7

Conclusions

In this thesis paper we compare conventional FRM with inset type FRM and result shows that the inset type FRM has high torque ability and small cogging torque. The amount of permanent magnet used in inset type FRM is 65% less than conventional FRM, and peak cogging torque of inset type FRM is 10% of conventional FRM.

Then we investigate the influence of major dimension of an inset type FRM for maximum output torque by finite element analysis. Stator back iron and rotor back iron has less effect on output torque. Stator teeth width has significant effect on output torque. Decreasing stator teeth width, decrease output torque. But increasing stator teeth width stator slot area is decreased. By decreasing stator back iron thickness we can increase stator slot area. Rotor pole arc has influence on cogging torque. Suitable choose of rotor pole arc reduce output torque ripple.

Reference

[1] Ming Cheng, K.T. Chau, and C.C. Chan, “Design and Analysis of a New Doubly Salient Permanent Magnet Motor,” IEEE Trans. Magn., vol. 37, no. 3, pp. 3012-3020, Jul. 2001.

[2] Y. Liao, F. Liang and T. A. Lipo, “A novel permanent magnet machine with doubly saliency structure”, Proc.IEEE IAS Annual Conf., 1992,pp.308-314.

[3] R.P. Deodhar, S. Andersson, I. Boldea, et al “The flux-reversal machine: a new blushless doubly-salient permanent-magnet machine,” Proc. IEEE IAS Annual Conf., 1996, pp.786-793.

[4] E. Hoang, A.H. Ben-Ahmed, J. Lucidarme, “Switching flux permanent magnet poly phased machines,” European Conf. Power Electronic and Applications, 1997, vol. 3, pp. 903-908.

[5] C. Wang, S.A. Nasar and I.Boldea, “Three phase flux reversal machine (FRM)”, IEE Proc. Elect. Power Appli, Vol. 146, pp. 139, 146, March `1999.

[6] T. H. Kim, “A Study on the Design of an Inset Permanent-Magnet-Type Flux-Reversal Machine,” IEEE Transaction on Magnetics, vol. 45, pp. 2859-2862, June 2009.

[7] P. J. Lawrenson, J. M. Stephenson, P. T. Blenkinsop, J. Corda, and N. N. Fulton, “Variable-speed switched reluctance motors,” *Proceedings B Electric Power Applications*, vol. 127, no. 4, pp. 253-265, July 1980.

[8] J. Oyama, T. Higuchi, T Abe, K. Haraguchi, E. Yamada, and F. Profumo, “Hybrid type novel switched reluctance motor,” *Proceedings of the 29th IEEE Annual Power Electronics Specialists Conference*, Fukuoka, Japan, May 2008, vol. 1, 857-863.

[9] Y. Liao, and T. A. Lipo, “A new doubly salient permanent magnet motor for adjustable speed drives,” *Electric Machines and Power Systems,* vol. 22, no. 2, pp. 259-270, February 1994.

[10] M. M. Radulescu, C. Martis, and I. Husain, “Design and performance of a small doubly-salient rotor-permanent-magnet motor,” *Electric Power Components and Systems,* vol. 30, no. 8, pp. 823-832, August 2002.

[11] Y. Liao, and T. A. Lipo, “A new doubly salient permanent magnet motor for adjustable speed drives,” *Proceeding of International Symposium on Power Electronics, Electrical Drives, Automation and Motion,* Positano, Italy, May 1992, pp. 415-420.

[12] R. P. Deodhar, S. Andersson, I. Boldea, and T. J. E. Miller, “The flux-reversal machine: a new brushless doubly-salient permanent-magnet machine,” *IEEE Transactions on Industry Applications,* vol. 33, no. 4, pp. 925-934, July/August 1997.

[13] S. E. Rauch, and L. J. Johnson, “Design principle of flux-switch alternators,” *Transactions of the AIEE Part III: Power Apparatus and Systems,* vol. 74, no. 3, pp. 1261-1268, December 1955.

[14] D.G Dorrel, I Chindurzha and F. Butt “Operation, theory and comparison of Flux Reversal Machine- Is it a viable position”,Int. Conf. Power Electronics and Drives, vol.1, pp.253-258, 2003.

[15] R.Krishnan “Permanent Magnet Synchronous and Brushless DC motor drives”, CRC press, 2010.

[16] I. Boldea, C. Wang, and S. A. Nasar, “Design of a three phase flux reversal machine,” Electrical Machine and Power System, vol. 27, no. 8, pp. 849–863, Aug. 1999.

[17] David Meeker,“Finite Element Method Magnetics." *User’s Manual*: Oct 16, 2010.

[18] Heung-Kyo Shin, Tae Heoung Kim, and Cherl-Jin Kim, “Demagnetization Characteristic Analysis of Inset-Type-Flux- reversal Machines”, 15th Int. Conf. Electric Machines and System, pp. 1-4, 2012.

[19] Boldea, J. Zhang, and S. A. Nasar, “Theoretical characterization of flux reversal machine (FRM) in low-speed servo drives-the pole-PM configuration,” IEEE Transactions on Industry Applications, vol.38. no. 6, November/December 2002.

[20] R. Ruse, “Calculation methods for a transverse flux reluctance motor,” in Proc. OPTIM 2000, vol. 2, Brasov, Romania, pp. 387-392.

[21] Boldea, I. ; Tutelea, L. ; Topor, M., “Theoretical Characterization of Three Phase Flux Reversal Machine with Rotor-PM Flux Concentration”, 13th Int. Conf. OPTIM, pp.472-476, 2012.

[22] More, D.S., Fernandes, B.G.: ‘Analysis of flux-reversal machine based on fictitious electrical gear’, IEEE Trans. Energy Convers., 25,(4), pp. 940–947, 2010.

[23] Nobuyuki Naoe,’ Voltage compensation of permanent magnet generator with capacitor”,Proc. Of IEEE electrical Machines and drives.,pp.wb2.14.1-wb2.14.3,1997.

[24] Vandana R and B.G. Fernandes, “Mitigation of voltage regulation problem in flux reversal machine”, IEEE Energy conversion Congress and Exposition (ECCE), pp.1549-11554, 2011.

[25] Ming Cheng,K.T.Chau.C.C.Chan."Design and Analysis of a New Doubly Salient Permanent Magnet Motor". IEEE Transactions on Magnetics, vol 37,No.4,July 2001.

[26] Sarlioglu.B and Lipo,T.A., “Assessment of Power Generation capability of Doubly salient Permanent Magnet Generator”, IEEE- International Electric Machines and Drives Conference, pp.9-12, Scattle, Washington, May 1999.

[27] Sarlioglu,B., Zhao,Y., Lipo,T.A., "A Novel Doubly Salient Single Phase Permanent Generator", IEEE IAS, Annual Meeting, Denver, Co.2-6,1994.

[28] Wang. C. X., Boldea. I., Nasar. S. A., “Characterization of three phase flux reversal machine as an automotive generator”, IEEE Trans. on energy conversion, Vol. 16, No. 1, pp. 74-80, 2001.

[29] H.Bahrami, M.Mirsalim, M.Mirzaei, H.Bahrami, “A Novel High-Speed Flux Reversal Alternator”,3rd IET Int. Conf. Power Electronics, Machines and Drives, pp. 212-215, ISBN- 0-86341-609- 8, April 2006.

[30] C.Wang, A. S. Nasar, and I. Boldea, “High speed control scheme of flux reversal machine,” in Proc. IEMD’99, May 9–12, 1999, pp.779- 781.